JOURNAL OF GEOPHYSICAL RESEARCH, VOL. 97, NO. D8, PAGES 8015–8034, MAY 30, 1992

Particle Size Distributions in Arctic Polar Stratospheric Clouds, Growth and Freezing of Sulfuric Acid Droplets, and Implications for Cloud Formation

J. E. DYE,[1] D. BAUMGARDNER,[1] B. W. GANDRUD,[1] S. R. KAWA,[2] K. K. KELLY,[2]
M. LOEWENSTEIN,[3] G. V. FERRY,[3] K. R. CHAN,[3] AND B. L. GARY[4]

Particle size and volume measurements obtained with the forward scattering spectrometer probe (FSSP), model 300 during January and February 1989 in the Airborne Arctic Stratospheric Experiment are presented and used to study processes important in the formation and growth of polar stratospheric cloud (PSC) particles. Comparisons of the observations with expected sulfuric acid droplet deliquescence suggest that in the Arctic a major fraction of the sulfuric acid droplets remain liquid until temperatures at least as low as 193 K. Arguments are presented to suggest that homogeneous freezing of the sulfuric acid droplets might occur near 190 K and might play a role in the formation of PSCs. The first suggestion of nitric acid trihydrate (NAT) particles appears near saturation ratios of HNO_3 with respect to NAT of 1 (about 195 K) as an enhancement of the large particles on the tail of the sulfuric acid droplet size distribution. The major increases in number and volume indicative of the main body of the NAT cloud are not seen in these Arctic investigations until 191 to 192 K, which corresponds to an apparent saturation ratio of HNO_3 with respect to NAT of about 10, unlike the Antarctic where clouds were encountered at saturation ratios near 1. A decrease in the number of particles was observed in regions in which the airmass was denitrified, i.e. NO_y, the sum of all reactive nitrogen species, was reduced. This was especially true for the larger particles on the upper tail of the sulfate size distribution. The loss of these largest particles supports the idea that denitrification may be the result of the preferential nucleation and growth of NAT on only the largest sulfate particles, which then sediment out of the airmass.

1. INTRODUCTION

Since the discovery from satellite extinction measurements [*McCormick et al.*, 1982] that polar stratospheric clouds (PSCs) occur frequently in the winter polar stratosphere, interest has shifted in just a few years from that of a scientific curiosity to one of major environmental significance. It is now clear that PSC particles act as catalytic surfaces for heterogeneous reactions that can lead to ozone destruction [*Solomon et al.*, 1986; *McElroy et al.*, 1986; *Jones et al.*, 1990]. The initial hypothesis of *Steele et al.* [1983], which followed earlier work of *Hallett and Lewis* [1967] on nacreous clouds, suggested that PSC particles were formed by the condensation of water vapor onto frozen sulfuric acid droplets. This proved incorrect when observations showed that the extinction expected for ice particles was too large to match the measured extinction [*Hamill et al.*, 1986] and that the particles formed at temperatures warmer than the frostpoint, the temperature at which saturation with respect to ice occurs [*Poole and McCormick*, 1988*a*]. *Toon et al.* [1986] and *Crutzen and Arnold* [1986] independently suggested that condensation of nitric acid, particularly nitric acid trihydrate (NAT), could occur at temperatures several degrees warmer than the frostpoint. Laboratory studies by *Hanson and Mauersberger* [1988] mapped the saturation vapor pressure curves of HNO_3 and H_2O over NAT and evaluated the likelihood of NAT formation in the polar regions. Subsequently, observations have shown that the particles do contain nitric acid [*Fahey et al.*, 1989; *Gandrud et al.*, 1989; *Pueschel et al.*, 1989; *Arnold et al.*, 1989; *Hofmann et al.*, 1990; *Schlager et al.*, 1990]. Airborne lidar measurements [*Poole and McCormick*, 1988*a*] showed that there are two stages in the observed backscatter, apparently associated with two kinds of particles. They found that the first stage, now referred to as type I particles, appeared in the Arctic at temperatures near 195 K, which is several degrees warmer than the frostpoint of about 188 K. Accumulating evidence shows the likelihood that type I particles are NAT [see *Kawa et al.*, this issue], although there is some uncertainty in the composition and whether or not the particles are crystalline, or amorphous or perhaps even liquid with a composition close to that of NAT. In this paper we will refer to the type I particles as NAT. They found that the second stage, type II particles, exhibit significantly larger backscatter and appear at temperatures colder than the frostpoint. They are thought to be predominantly ice.

Most scenarios for the nucleation and growth of PSC particles assume that nucleation followed by co-condensation of HNO_3 and H_2O occurs on already frozen sulfuric acid droplets to form NAT particles. However, there has been some discussion of the possibility that the nitric acid containing particles are supercooled liquid [e.g. *Hanson*, 1990] composed of a ternary mixture of H_2SO_4-HNO_3-H_2O [*Crutzen et al.*, 1988; *Hofmann and Deshler*, 1990]. *Crutzen et al.* [1988] suggest that a requirement for the formation of solid NAT particles is that the sulfuric acid particles are frozen. *Poole and McCormick* [1988*b*] assumed that there was not a barrier for nucleation of the NAT on the frozen sulfuric acid droplets, while *Poole et al.* [1990], *Wofsy et al.* [1990], and *Peter et al.* [1991] explore the effects of different free energy barriers (contact angles) on the nucleation of NAT particles. In the models of *Poole et al.* and *Wofsy et al.*, curvature effects and cooling rate as well as energy barrier were found to control the number of particles

[1]National Center for Atmospheric Research, Boulder, Colorado.
[2]NOAA Aeronomy Laboratory, Boulder, Colorado.
[3]NASA Ames Research Center, Moffett Field, California
[4]Jet Propulsion Laboratory, Pasadena, California.

Paper number 91JD02740.
0148-0227/92/91JD-02740$05.00

which can nucleate and grow. These models suggest that with high cooling rates (more than about 5 K per day) the rate at which HNO_3 condenses is small compared to the rate of increase of available HNO_3 vapor (i.e., the difference between the saturation vapor pressure at the surface and the ambient partial pressure) and thus large supersaturations develop which in turn activate most of the frozen sulfuric acid droplets. They also suggest that tens of minutes are required for the formation of PSC particles in an air parcel moving with the wind, although the clouds themselves can persist for hours or days. Like wave clouds, particles form at the leading edge, move through the cloud following the air motion except for slight sedimentation, and dissipate at the trailing edge of the cloud. For cooling rates less than about 1 K per day the rate of condensation comes closer to balancing the HNO_3 available for growth and fewer NAT particles are nucleated, resulting in larger particles. *Hofmann et al.* [1989*a*] believe that the micron-sized particles which they observed in Antarctica are the result of growth in airmasses which experienced slow cooling rates. *Salawitch et al.* [1989] suggest that the sedimentation of these larger NAT particles causes removal of nitric acid from the airmass, i.e., denitrification, which has important consequences for ozone destruction.

During the Airborne Arctic Stratosphere Experiment (AASE), particle measurements were made from the NASA ER–2 with a forward scattering spectrometer probe (FSSP) model 300 [*Baumgardner et al.*, this issue: *Dye et al.*, 1990*a*] which was designed to provide improved measurements in PSCs. Measurements obtained with the FSSP 300 on the January 24, 1989, flight of the ER–2 were presented by *Dye et al.*, [1990*b*]. The key features from this flight were that the first appearance of PSC particles occurred near apparent saturation ratios of nitric acid with respect to NAT of about 1, but the main increase in number and volume of particles was not detected until the apparent saturation ratio of HNO_3 with respect to NAT reached about 10. *Gandrud et al.* [1990] presented observations from the January 30, 1989 flight of the ER–2 during which particles > 4 μm diameter were observed and concluded that these large particles were probably type II particles and had fallen from above the ER–2 altitude.

Although we have learned much about PSCs in just a few years, many questions remain about the chemical composition of the particles, the nucleation and growth of the particles, the size and surface area distribution of the particles in different environmental conditions, and the factors which control the number and hence size of the particles. The purpose of this paper is to present in more detail the evolving size distributions from each of the ER–2 flights in which PSC particles were detected and to investigate mechanisms responsible for the formation of the particles. We first examine the growth and dilution of sulfuric acid droplets and the temperature at which they may freeze. This is followed by an examination of the conditions in which NAT particles are first detected and the conditions present when the ER–2 enters the main type I PSC cloud. Observations of larger particles, presumed to be type II ice particles, are related to the temperature structure near and above the ER–2. We then explore changes in the particle size distribution in regions in which denitrification has occurred. Finally we discuss the possible role of the homogeneous freezing of sulfuric acid droplets in addition to cooling rate as a factor in determining the number of sulfate particles which can serve as nuclei to form NAT. The FSSP 300 measurements are also used in conjunction with NO_y and H_2O measurements in *Kawa et al.* [this issue] to investigate the composition of PSC particles.

2. Overview of the Flights

Fourteen flights were made by the ER–2 from Sola Airfield near Stavanger, Norway, during the AASE. *Turco et al.* [1990] give an overview of the project and the parameters measured from the ER–2. The results which we present here are primarily from the seven flights in which PSCs were encountered. We also show measurements from the flight of January 3, 1989 (hereafter we will use the notation 890103), in which the aircraft entered the vortex and the temperature dropped to 194 K but there was no clear indication of PSC particles.

Most of the northbound legs of the flights were flown at a nearly constant potential temperature of about 440 to 460 K, at nominal pressures of 50 to 60 mbar (19 to 20 km). A typical pattern was to fly north along the coast of Norway to approximately 69° N latitude, then due north to a maximum latitude of about 78° near Spitzbergen. Shortly after reversing heading, the plane often descended to about 16 km altitude (about 120 mbar, potential temperature near 380 K) and reascended to fly another constant potential temperature surface back to Stavanger. The horizontal winds at the ER–2 altitude always had a significant westerly component. Thus the ER–2 flight tracks were not along the direction of airflow and the measurements do not allow us to examine particle evolution along parcel trajectories. Although the ER–2 did not fly a Lagrangian flight path, the day to day similarity in changes in the particle size distributions as temperature changes provides suggestions of what the Lagrangian evolution might have been.

3. Comments on the FSSP 300 Measurements

Before presenting the observations it is important to discuss some aspects of the FSSP 300 measurements. *Baumgardner et al.*, [this issue] discuss the operation of the probe and evaluate the limitations and uncertainties in the measurement of concentration and size. As they point out, accurate interpretation of measurements from the FSSP 300 requires knowledge of the particle index of refraction and shape.

In this paper we are mainly investigating the transitions from liquid or solid sulfuric acid droplets to nitric acid containing particles, which are probably NAT in the solid phase. However, we are uncertain if they are crystalline or amorphous or even liquid and what the exact composition is. Additionally, at temperatures near or below the frostpoint some of the particles are likely to be predominantly ice. Thus we are concerned with a range of indices of refraction ranging from about 1.31 for ice, to 1.40 for dilute sulfuric acid droplets near 195 K, to perhaps 1.50 for crystalline NAT particles, which *Toon et al.* [1990] have estimated from the Lorentz–Lorenz relation based on a NAT density of 1.62 g cm^{-3} [*Taesler et al.*, 1975]. Because we are primarily concerned with the sulfate and NAT particles in this paper, we have used an index of refraction of 1.40. We show below that the shape of the observed size distributions is such that most

of the particle volume (mass) in the PSCs which we observed is between 0.7 and 1 μm diameter. In Figure 1 we see that for an index of refraction of 1.4 or 1.5, from about 0.7 to 1.0 μm diameter the scattered intensity and hence size and particle volume is almost the same. To check for effects on particle mass, the PSC particle measurements for 890124, a day with a well developed PSC, were processed using size limits defined for indices of refraction of both 1.4 and 1.5. The difference in calculated volumes for these two indices of refraction were less than 5%. Thus the choice of 1.40 should not alter any of the conclusions which we draw herein or in the companion paper by *Kawa et al.* (this issue) which uses FSSP 300 measurements to examine composition of the nitric acid containing particles. The use of 1.40 also allows accurate sizing of the sulfuric acid droplets which dominate the small particle measurements.

Following the procedure explained in *Baumgardner et al.* [1989] and *Dye et al.* [1990*a*] for the FSSP 300, we have regrouped the 31 original channels into 19 channels to help remove ambiguities arising from oscillations in the Mie scattering curves and misfit at the two gain stages of the pulse height analyzer. The size limits, midpoints, and channel widths for the 19 bins used herein are shown in Table 1. These channel definitions have been corrected for the 200 m s^{-1} airspeed of the ER–2 [*Baumgardner et al.*, this issue] and are the same as given in *Dye et al.*, [1990*a*] except that channels 12 and 13 in Dye et al. have been combined into one channel to further smooth the effects of the Mie peaks. The limits of each channel assume the particles to be spherical, which for NAT particles seems reasonable based on the formvar replicas of particles collected on the impaction wires for 890116 and 890124 which show circular impressions [*Pueschel et al.*, this issue]. Additionally, light scattering from nonspherical particles is nearly the same as from spherical particles of the same volume diameter when the size parameter, $\pi D/\lambda$, (where D is particle diameter and λ is wavelength) is < 5 [*Zerull*, 1976]. For the 633 nm wavelength of the HeNe laser used in the FSSP, this corresponds to about 1 μm.

For particles between about 1 and 5 μm diameter the oscillations in the Mie scattering curve are pronounced (Figure 1), limiting sizing resolution and accuracy regardless of index of refraction. Above 5 μm we see in Figure 1 that the size is not a strong function of the index of refraction. However, most of the particles larger than 4 μm observed by the FSSP are likely to be ice–like particles, as discussed later. Replicas of these particles in the Antarctic by *Goodman et al.* [1989] found average aspect ratios of 2 to 3. Because the light scattered from nonspherical, large particles is less than that from a sphere of equivalent volume diameter [*Zerull*, 1976], the volumes measured by the FSSP for the large particles may be underestimated.

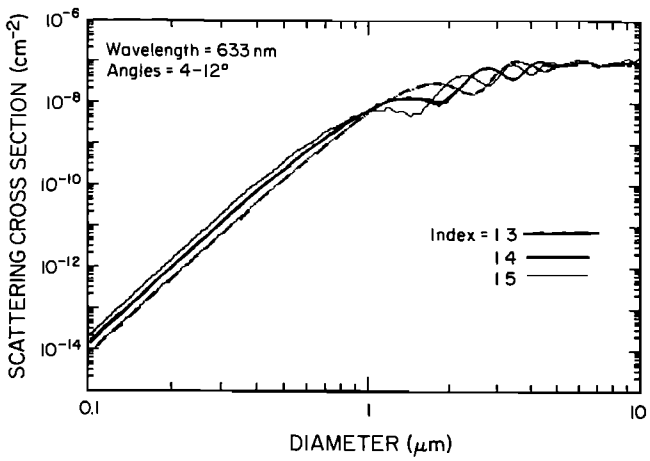

Fig. 1. Scattering cross section as a function of particle diameter for the indicated indices of refraction for the angular aperture and wavelength of the FSSP 300.

TABLE 1. FSSP 300 Regrouped Channel Limits

Channel		Size Limits,	Midpoint,	Width,
Grouped	Original	microns	microns	microns
1	1	0.37–0.42	0.395	0.05
2	2	0.42–0.47	0.445	0.05
3	3	0.47–0.51	0.490	0.04
4	4	0.51–0.55	0.530	0.04
5	5	0.55–0.60	0.575	0.05
6	6	0.60–0.65	0.625	0.05
7	7	0.65–0.70	0.675	0.05
8	8–9	0.70–0.89	0.795	0.19
9	10–11	0.89–0.99	0.940	0.10
10	12	0.99–1.08	1.035	0.09
11	13–14	1.08–2.15	1.615	1.13
12	15–19	2.15–3.97	3.060	1.82
13	20–21	3.97–6.88	5.425	2.91
14	22	6.88–8.27	7.575	1.39
15	23	8.27–9.78	9.025	1.51
16	24–25	9.78–11.53	10.655	1.75
17	26–27	11.53–13.53	12.530	2.00
18	28–29	13.53–15.51	14.520	1.98
19	30–31	15.51–23.67	19.590	8.16

NOTE: In this table the 31 original channels have been regrouped into 19 to remove ambiguities in the Mie scatter curve. This grouping is for an index of refraction of 1.40 and does not apply to all indices of refraction.

Another uncertainty which needs discussion is the sample area of the FSSP 300, because it directly influences the calculated concentration and derived surface area and volume. The sample area used herein as well as in earlier results presented by *Dye et al.*, [1990*a*,*b*] and *Gandrud et al.*, [1990] is 0.05 mm^2. This value was derived from intercomparisons with other particle instruments on flights on the National Center for Atmospheric Research (NCAR) Sabreliner specifically for the purpose of determining the sample volume and was in basic agreement with the theoretically expected value. Additionally, volumetric calibrations of the sample area performed in the laboratory at Particle Measuring Systems just before the AASE gave similar values to that quoted above. Very recent laboratory tests to check for electronic imbalance at low temperatures continue to support the value of 0.05 mm^2. *Baumgardner et al.* [this issue] discuss the sample volume determination in more detail and estimate the uncertainty to be about +/- 25 %.

Most of the observations presented below are 120 or 300 s averages of the particle measurements. For the above sample area and an airspeed of 200 m s^{-1}, the expected statistical uncertainty for 120 s averages of concentrations of 10, 1, 0.1, and 0.01 cm^{-3} would be +/- 0.9, 2.9, 9.1, and 29 %, respectively. For 300 sec averages, the statistical uncertainties for the above concentrations decrease to +/- 0.5, 1.7, 5.3, and 16.7%, respectively.

During the flights prior to 890116 the first channel of the FSSP had counts which were considerably in excess of background. Laboratory tests showed that the noise was probably a result of shifts in laser alignment caused by thermal gradients at the very cold temperatures encountered in the stratosphere. Better techniques for optical alignment, which we developed during the project, corrected this problem for the 890116 flight and thereafter. Even for the early flights, there was no evidence in the data that the counts extended into the second and third channels. Because the slope of the Mie scattering curve is so steep for small particles, the voltage width of the first channel spans a factor of almost 4, which except for severe noise problems, limits noise in most of the Particle Measuring System instruments to the first channel. As discussed in *Dye et al.* [1990*b*], examination of size distributions during the later part of the experiment when noise was not a problem showed that the part of the sulfuric acid particle distribution seen by the FSSP 300 could be reasonably approximated by an exponential distribution with a slope of about -6. We have corrected the data in channel 1 shown here for 3 of the 8 flights (890103, 890112, and 890124 after 47200 s UT) by predicting a concentration for channel 1 assuming an exponential distribution based on the average concentration of channels 2 and 3. This correction was applied only when the measured concentration in channel 1 was more than the predicted one. We estimate that after correction, the uncertainty due to the noise on these days is less than 5 % in the total concentration measured by the FSSP 300 and much less in the calculated volume. Even if we excluded the first channel entirely, the conclusions reached in this paper would remain the same.

4. Particle Measurements and Interpretation

A summary of the FSSP 300 measurements for each of the days in which the ER-2 flew in PSCs and for 890103 which had a minimum temperature of 194 K are presented in Figure 2. In addition to total concentration, in these figures we also display the concentrations in three broad size categories as a convenient way of showing changes in the size distribution which roughly, but not strictly, correspond to changes in particle type. The three categories are (1) the sum of the concentrations of particles in the size intervals 0.37 to 0.6 μm diameter which, when the ER-2 is outside of PSCs, corresponds to the larger particles of the sulfate distribution (which is all that is seen by the FSSP); (2) 0.6 to 4.0 μm, which contains primarily NAT particles; and (3) 4.0 to 23.7 μm, which are the largest particles and are indicative of type II particles, i.e., ice growth. Inside PSCs the first category may also contain NAT particles and the second category may contain a few type II particles. The heavy solid lines in Figure 2 show the ambient temperatures. The heavy horizontal dashed curves near 195 to 196 K show the temperatures needed to reach saturation of HNO_3 over NAT based on the *Hanson and Mauersberger* [1988] relationship, the observed pressure and water vapor mixing ratio [*Kelly et al.*, 1990] and the assumption of 10 ppbv of HNO_3 in the gas phase. These curves correspond approximately to the temperature at which NAT formation might be expected to occur (see Section 4b for further discussion).

4.1. Relationship Between N_2O and Sulfate Particles

Previous studies by *Wilson et al.* [1989, 1990] show a relationship between the condensation nuclei (CN) concentration, which are assumed to be entirely sulfate particles, and N_2O mixing ratios. Their measurements show that inside the vortex, when N_2O decreases the number and modal size of the sulfate particles also decreases in response to changes in airmass. Similarly, the FSSP which detects the larger sulfate particles shows a decrease in concentration and a shift to smaller sizes when N_2O decreases in the vortex. Figure 2 of *Loewenstein et al.* [1990] shows that at ER-2 flight altitudes during the AASE, a value of 175 parts per billion by volume (ppbv) of N_2O is a good demarkation between airmasses inside and outside of the vortex. Based on their findings, we have used decreases in N_2O from greater than 200 to less than about 150 ppbv, which are usually quite sharp, to identify the vortex boundary. The short, vertical bars near the top of each concentration plot in Figure 2 show the location of the boundary defined in this manner. TA with an arrow near the center of each plot shows the time at which the ER-2 turned around to start heading south. The FSSP 300 measurements frequently show decreases in concentration (for example, 890103, 890112, 890119 in Figure 2) at the N_2O boundaries. This is particularly true for the 0.6 to 4.0 μm category of particles. Although changes in sulfate particle numbers and volume seen by the FSSP inside the vortex are often correlated with changes in N_2O, outside the vortex the size distribution is less sensitive to N_2O changes. In the following section we will use changes in N_2O as indicators of changes in airmass [*Loewenstein et al.*, 1990] and thus, as a guide to when particle size distributions are changing due to changes in airmass.

4.2. Growth and Dilution of Sulfuric Acid Droplets

Dye et al., [1990*b*] suggested that the increase in particle volume observed for the 890124 case, before temperatures were cold enough to expect NAT formation (30600 to 33000 UT s), might be the result of deliquescence of the sulfuric acid droplets. To examine this possibility, the volume of particles measured by the FSSP for particles < 4 μm diameter is plotted as a function of temperature for each of the days in Figure 3. The plots include only the northbound portion of each flight because this was flown at approximately constant potential temperature. By using the fractional increases in size given by *Steele and Hamill* [1981] in their Table 1 for 3 x 10^{-4} mb H_2O (5 ppmv at 60 mbar total pressure) and a given particle size distribution, we can determine the fractional increase in volume which would be expected for growth of the sulfuric acid droplets as they come to equilibrium with the ambient water vapor pressure as temperature decreases, assuming that the sulfuric acid droplets are of uniform composition.

Because the FSSP sees only the large tail of the sulfuric acid droplet spectrum, the number of the sulfate particles which the FSSP counts should increase as the sulfate parti-

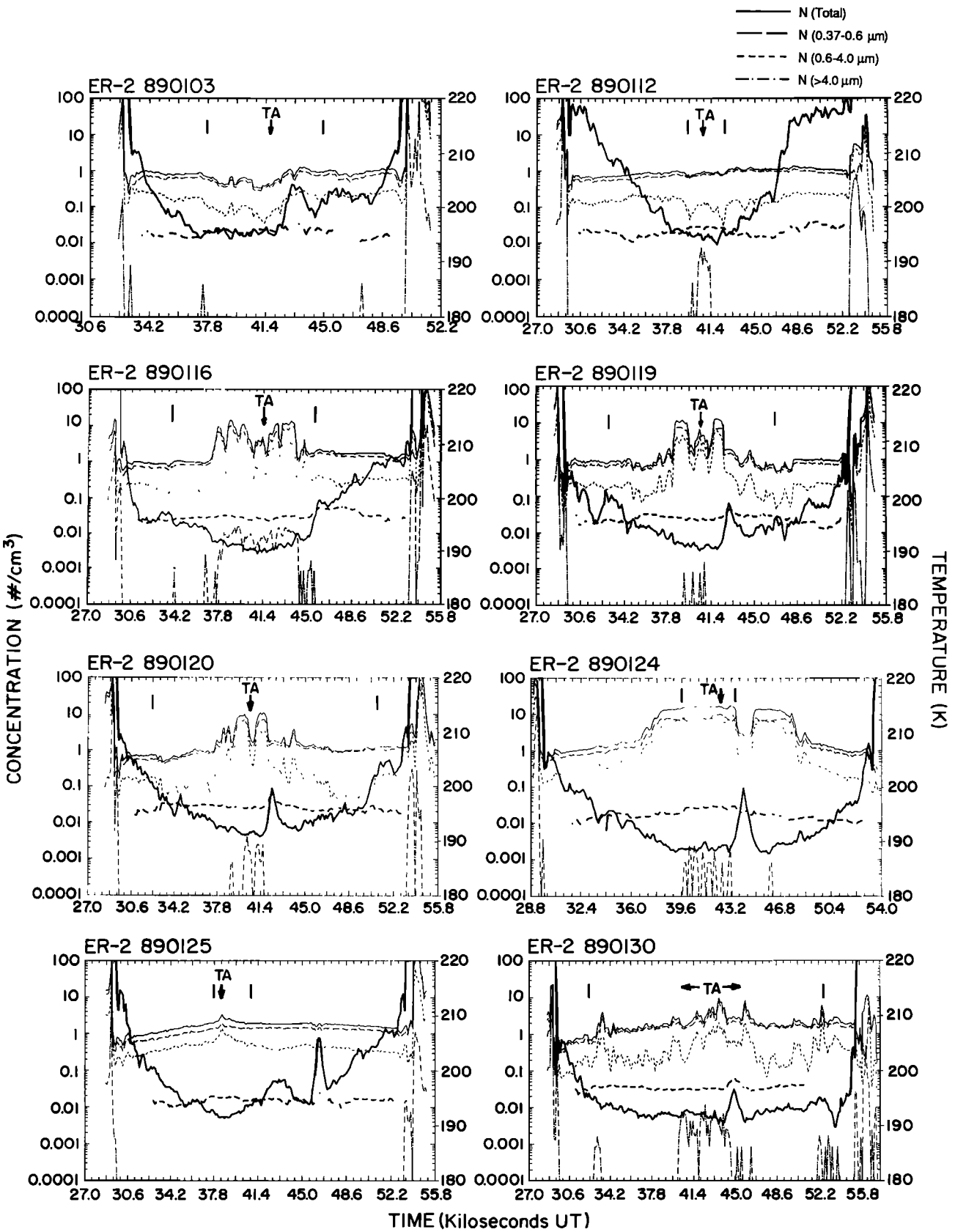

Fig. 2. Total particle concentrations and concentrations in the indicated size categories for 120 s averages of the FSSP 300 measurements for eight flights of the ER-2. The ambient temperature is shown by the heavy solid curve with scales on the right of each plot. The heavy horizontal dashed curve near 195 to 196 K shows the temperature at which HNO_3 saturation over NAT occurs (see text). The short vertical lines at the top of each plot show the vortex boundary determined from N_2O measurements, and TA the turnaround time of the ER-2.

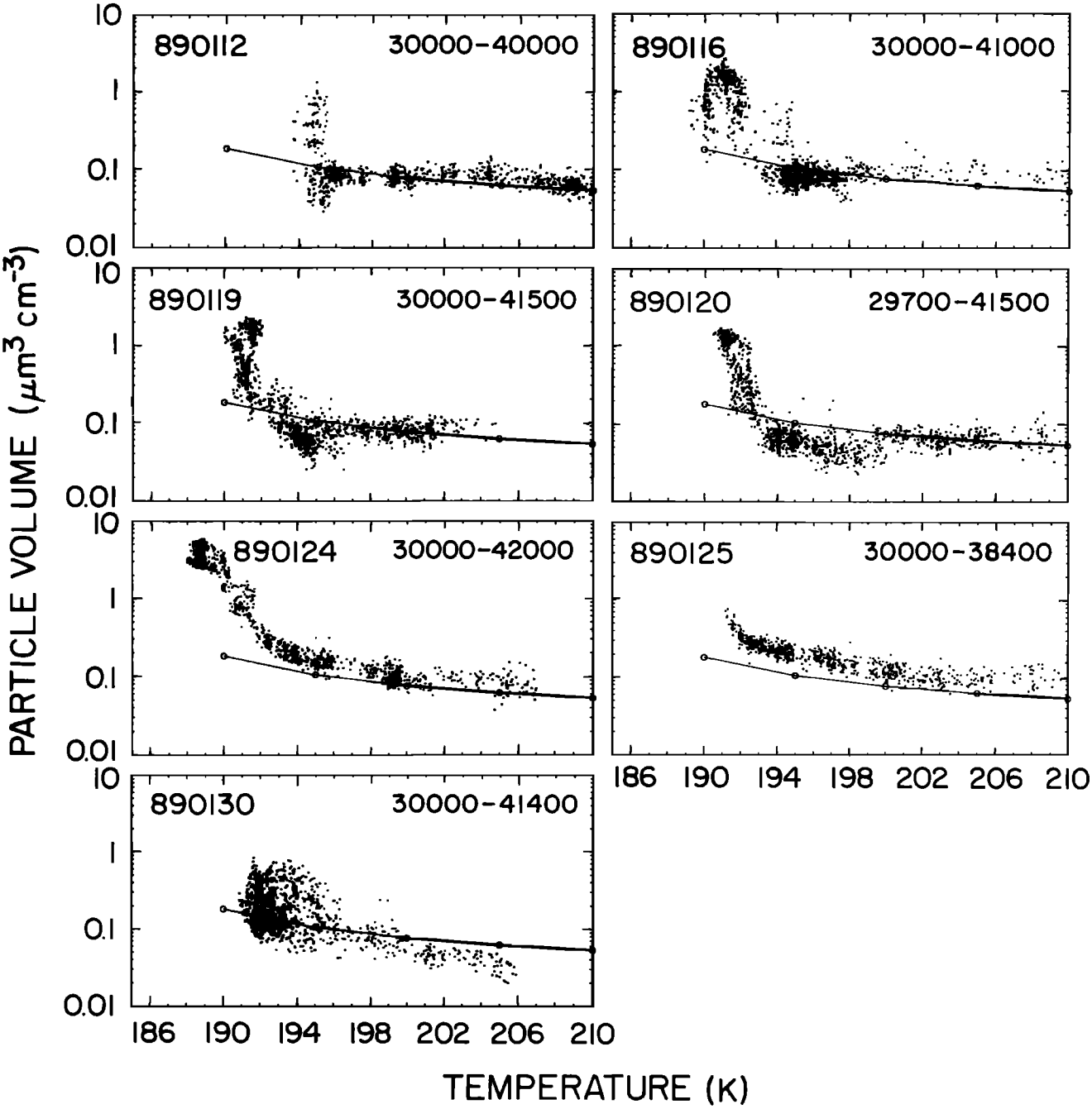

Fig. 3. Particle volume measured by the FSSP 300 for particles < 4 μm diameter plotted as a function of ambient temperature. The solid curve shows the particle volume expected from deliquescence of liquid sulfuric acid droplets (see text). Observation times in UT seconds are shown in the upper right of each plot.

cles grow by absorbing more H_2O in response to decreasing temperature. Therefore, for comparison with observations we examined the growth of a changing, truncated lognormal distribution. Following *Feingold and Levin* [1986], the truncated form (indicated by t) for the nth moment of a lognormal distribution can be expressed as

$$I_n^t = \int_{D_{min}}^{D_{max}} f(D)\, D^n\, dD \qquad (1)$$

where $f(D)$ is the lognormal probability distribution for diameter D given by

$$f(D) = \frac{1}{\sqrt{(2\pi)}\, D ln\sigma}\, exp\left[\frac{-ln^2(D/D_g)}{2\, ln^2\sigma}\right]$$

After integration and determining the coefficients for volume, we have

$$I_3^t = \frac{4}{3}\pi\, N_o\, D_g^3\, exp\left(\frac{9}{2}\, ln^2\, \sigma\right)$$

$$[\text{erf}\,(Y_{max}) - \text{erf}\,(Y_{min})] \qquad (2)$$

where erf is the error function defined by

$$\mathrm{erf}(z) = \frac{1}{\sqrt{(2\pi)}} \int_{-\infty}^{z} e^{-t^2/2} dt$$

$$Y_{max} = \frac{ln(D_{max}/D_g) - 3ln^2\sigma}{ln\ \sigma}$$

and

$$Y_{min} = \frac{ln(D_{min}/D_g) - 3ln^2\sigma}{ln\ \sigma}$$

The lognormal size distribution which we used for comparison was based on a lognormal fit to the sulfate number distribution (J. C. Wilson, personal communication, 1991) measured by the CN counter and the Passive Cavity Aerosol Spectrometer (PCAS) for 890124 between 32000 and 33000 UT s, when temperature was relatively constant at about 200 K. The parameters of the distribution are geometric mean diameter D_g = 0.184 μm, standard deviation σ = 1.80, and concentration N_o = 15 cm^{-3}. The N_o of this distribution was adjusted to fit the concentrations measured by the FSSP inside the PSC on this day and is larger than the measured CN concentration (6 cm^{-3}). This same distribution is used for comparison with the observations on all days.

The calculated volumes expected as temperature decreases from 210 to 190 K are shown as open circles at 5 K intervals in Figure 3. The same curve is shown for all days. Even though the calculated fractional changes in volume for 890124, agree with the observed fractional increases, the calculated volumes are less than the measured volumes. This results because the lognormal fit of the number distribution underestimates the number of large particles on the tail of the distribution. This departure in volume at the large sizes is clearly seen in Figure 12 of J. C. Wilson et al. (Stratospheric sulfate aerosol in and near the northern hemisphere polar vortex: Morphology of the sulfate layer, size distribution, and effect of denitrification, submitted to *Journal of Geophysical Research*, 1991; hereinafter referred to as submitted manuscript, 1991). Also, because the airmass and therefore the sulfate size distribution was not the same on each day, there is a day to day variation between the calculated volumes (which are based only on the 890124 PCAS fit) and the particle volumes measured by the FSSP between 190 and 210 K. For evaluating possible deliquescence of the sulfate particles, we are most interested in the fractional changes of volume with temperature since it is thought [*Steele and Hamill*, 1981] that the composition of the sulfate particles is uniform for all sizes.

It is apparent in Figure 3 that the observed data from 210 to 195 K on some days, e.g., 890124, 890125, and 890130, show a gradual increase in volume with decrease in temperature and others do not. After close examination of the N_2O, H_2O, and temperature data in conjunction with the particle data, we found that as temperature decreased from 210 to 195 K on 890112, 890116, 890119, and 890120, N_2O showed large decreases indicating changes in airmass. On these days changes in particle distributions from the changing airmass apparently obscure the increases in volume which are expected due to deliquescence of liquid droplets. For example, on 890112 and 890116 N_2O decreased from about 220 to 125 ppbv during the time period of the plots in Figure 3. However, on 890124, 890125, and 890120 between 33200 and 37200 s, and 890119 between 32400 and 34800, N_2O was relatively constant and measured fractional increases in volume (Figures. 3 and 4) are consistent with those expected from growth predicted by *Steele and Hamill* [1981]. For the subsets of time on 890120, N_2O was 150 +/- 20 ppbv and on 890119 was 200 +/- 10 ppbv. The lower values of particle volume for 890120 compared to 890119 for this subset are a result of lower aerosol concentrations at the lower N_2O mixing ratios in the vortex. Figure 4 shows that although the total volumes are different for the time subsets on the two days the observed fractional increases are similar, as would be expected for particles of uniform composition. Thus, the observations support the calculations of Steele and Hamill on the changing composition of the stratospheric sulfate particles at these cold temperatures. At temperatures < 193 K when the ER-2 begins to enter PSCs, larger departures from calculated volumes begin to occur.

It is important to note that if the sulfuric acid droplets were frozen, as has usually been assumed [e.g., *Poole et al.*, 1990 and *Wofsy et al.*, 1990], we would not expect an appreciable, gradual increase in volume as the temperature decreases from 210 K to the point at which NAT formation begins. Droplets in the liquid state can change composition by absorbing water and increasing in size to maintain equilibrium between the changing saturation vapor pressure at the surface and the partial pressure of the ambient water vapor. However, frozen droplets could not grow significantly by condensation of H_2O until the temperature drops below the frostpoint. Because the rate of collision of H_2SO_4 molecules with the surface is about 10^7 less than that of water, the droplets are probably undersaturated with respect to H_2SO_4 [*Steele and Hamill*, 1981]. They estimate that time scales for change in response to differing H_2SO_4 concentrations are probably months to a year. Significant growth by absorption of H_2SO_4 should not occur on the time scale of a PSC event.

Although frozen droplets would not be expected to grow by condensational growth from H_2O until the frostpoint is

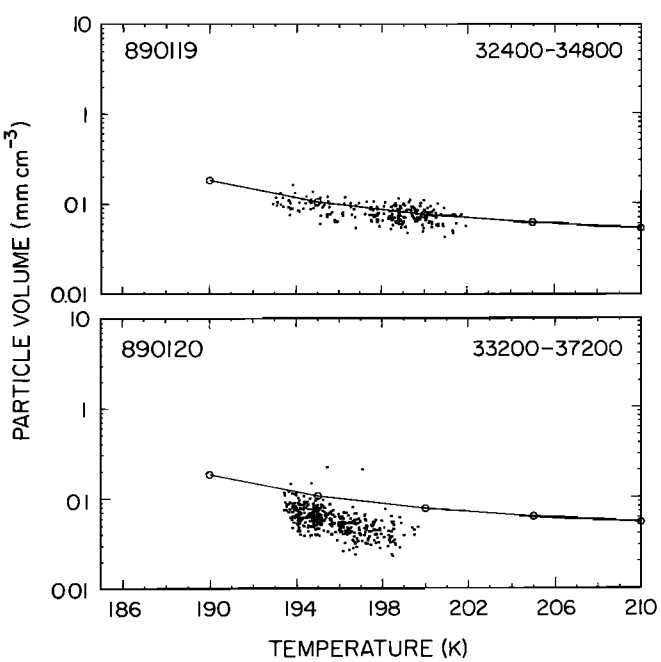

Fig. 4. As in Figure 3 for 890119 and 890120 for selected time periods when N_2O was relatively constant.

reached, at the time the droplets crystallize there could be an increase in volume due to the lower density of ice compared to water. The change in volume would depend upon the fraction of ice and different hydrates in the crystallized droplet. This increase in volume plus the change in refractive index might be an explanation for the enhancement of larger particles of the sulfate distribution seen by J. C. Wilson et al. (submitted manuscript, 1991).

The observations clearly show a gradual increase in observed volume (when N_2O is relatively uniform), which is in agreement with the expected growth due to deliquescence, leading us to conclude that most of the sulfuric acid particles are still liquid down to at least 193 K. This conclusion is supported by photomicrographs of imprints of particles impacted on impaction wires by *Pueschel et al.*, [this issue]. The shape and flattening of the impact craters suggest that the particles were liquid during collection (see their Figure 6). This finding is also supported by the laboratory studies of *Gable et al.* [1950], who found that even in bulk solutions large supercoolings of H_2SO_4 could occur which made it very difficult for them to nucleate the different hydrates. *Hofmann and Deshler* [1991] examined their measurements for evidence of deliquescence in Antarctica by using an exponential fit to their observed particle distributions. However, their measurements, which have less size resolution than the FSSP 300 measurements, had too much scatter to either confirm or preclude deliquescence.

4.3. *Homogeneous Freezing of Sulfuric Acid Droplets*

The laboratory studies of *Pruppacher and Neiburger* [1963] showed that solutes enhance the supercooling of pure water and that the resultant supercooling was approximately equal to the sum of the maximum supercooling for pure water plus the equilibrium freezing-point depression due to the solute. This and the work of *Gable et al.* [1950] led *Hallett and Lewis* [1967] to postulate that the supercooling of sulfuric acid droplets in the stratosphere could be very large and in their Figure 5 showed the maximum supercooling which they expected for different weight percentages of SO_3 in water. In Figure 5 we replot the maximum supercooling curve of Hallett and Lewis (converted to weight percentage of H_2SO_4 in water) superimposed on the equilibrium phase diagram for ice and the hydrates for sulfuric acid–water solutions adapted from *Steele et al.*, [1983] and *Gable et al.*, [1950]. Our figure also shows the equilibrium weight composition of a sulfuric acid droplet as a function of temperature after *Steele and Hamill* [1981] for H_2O partial pressures of 3×10^{-4} and 5×10^{-4} mbar (5 and 7 ppmv at 60 mbar). The sulfuric acid solution droplets can be supercooled with respect to ice and also supersaturated with respect to the sulfate hydrates. If one nucleates but not the other, the droplet can be mixed phase and this occurrence is a distinct possibility. Once the droplet begins to freeze, ice and various crystal hydrates will form as the solution becomes more and more concentrated, ultimately becoming a complicated mixture of ice and hydrates.

As an airmass cools, H_2SO_4 solution droplets will take on water and grow to maintain equilibrium. They can continue to grow and supercool, following the weight composition curve in Figure 5 for the appropriate water vapor mixing ratio, until they freeze. This can occur through heterogeneous nucleation, i.e., nucleation by a foreign body, or by homogeneous nucleation. The intersection of the weight percentage curve with the maximum supercooling curve in Figure 5 gives the approximate temperature at which homogeneous nucleation would be predicted to occur, based on Hallett and Lewis' work. For 5 ppmv at 60 mbar, the water vapor mixing ratio found by *Kelly et al.* [1990] in the Arctic, the predicted temperature of homogeneous nucleation is 189 K. For 7 ppmv it is 191 K. We speculate that the enhancements of the large particles on the tail of the sulfate particle distributions observed by J. C. Wilson et al. (submitted manuscript, 1991) may be due to the small fraction previously frozen by heterogeneous nucleation, but that most of the particles remain liquid until 193 K or colder and freeze homogeneously.

Once the sulfuric acid droplets are frozen, they will stay solid until they evaporate at temperatures above about 240 K [*Hamill and McMaster*, 1984]. However, it may take considerable time for all air parcels in the vortex to reach temperatures sufficiently cold for all of the particles to freeze. Note from Figure 2 that the volumes plotted for 890124 and 890125 in Figure 3 are outside of the vortex as are the 890119 data in Figure 4. However, the data in Figure 4 for 890120 are inside the vortex. The evidence suggests that deliquescence is occurring both in and out of the vortex.

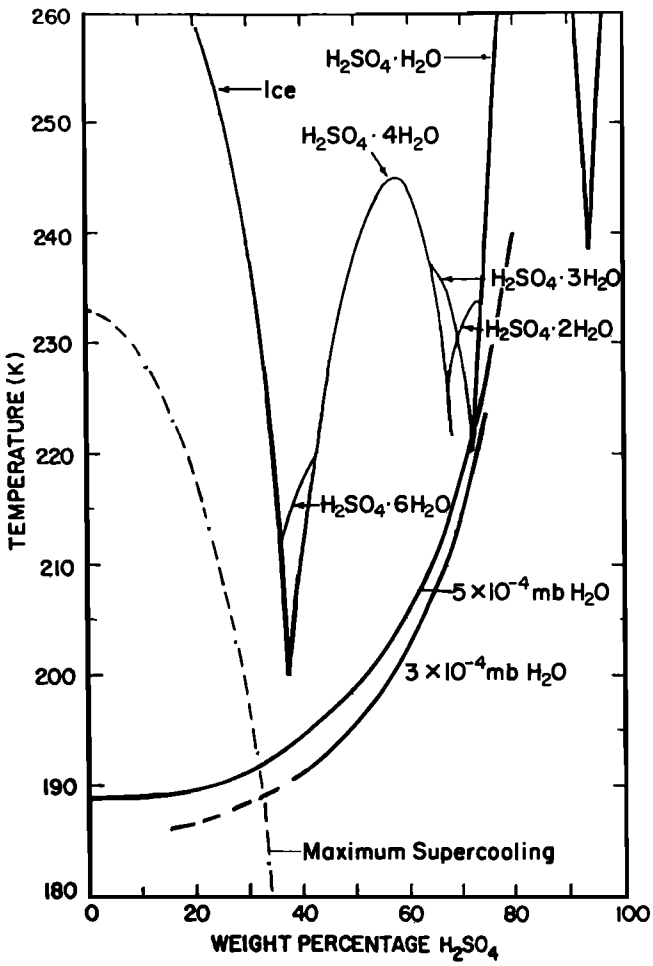

Fig. 5. Superposition of the freezing point diagram of the $H_2SO_4 - H_2O$ system from *Gable et al.* [1950]; composition of sulfuric acid droplets from *Steele et al.* [1983] for H_2O partial pressures of 3 and 5×10^{-4} mbar and maximum supercooling for H_2SO_4–H_2O solutions from *Hallett and Lewis* [1967].

Without direct experiments we can not conclusively determine the temperature at which homogeneous freezing occurs. Measurements presented here strongly suggest that the majority of the sulfuric acid droplets are liquid down to temperatures of at least 193 K, past the temperature at which PSC particle formation could begin. The discussion above suggests that it may be possible to supercool the droplets to approximately 190 K in conditions present during the AASE, although the transition to frozen droplets is not well known. *Crutzen et al.* [1988] also suggested that "once an air parcel has cooled to temperatures below 191 K the H_2SO_4/H_2O aerosol will most likely be solid," based on observations which show cirrus like particles near 191 K. The abrupt increases in particle volumes associated with entry into PSCs in Figure 3 occur near 191 to 192 K, which based on the above discussion is very near the temperature at which sulfuric acid droplets might freeze homogeneously. This correspondence suggests to us a possible link between the main occurrence of the observed polar stratospheric clouds and the homogeneous freezing of sulfuric acid droplets. This idea is combined into a conceptual model of PSC nucleation and growth in a later section.

4.4. *First Appearance of Particles Containing Nitric Acid*

The temperature at which NAT particles would be expected to be in equilibrium with the existing HNO_3 and H_2O vapor pressures for a given ambient pressure can be calculated from the relationship derived by *Hanson and Mauersberger* [1988] from their laboratory experiments. By ratioing the expected ambient vapor pressure of HNO_3 with the saturation vapor pressure from the Hanson and Mauersberger relationship, an apparent saturation ratio of HNO_3 with respect to the NAT particles can be calculated. In calculating this ratio we assume that the HNO_3 vapor pressure is the amount of NO_y predicted from the empirical, linear relationship between N_2O and NO_y observed for the polar regions (referred to as NO_y*) [*Fahey et. al.*, 1989; *Kawa et. al.*, 1990], where NO_y is the sum of all reactive nitrogen species. The apparent HNO_3 saturation ratio with respect to NAT then is the predicted HNO_3 vapor pressure, NO_y*, divided by the equilibrium saturation vapor pressure of HNO_3 over NAT. We will refer to this ratio as NO_y^*/HNO_3sat. This saturation ratio provides a useful guide as to when saturation with respect to NAT might occur and particle growth may be expected. However, it is larger than the true supersaturation [*Poole et al.*, 1990; Wofsy et al., 1990], because a large fraction of the available HNO_3 may have been deposited on particles as NAT, HNO_3 may have been lost from the air parcel due to prior denitrification, and because not all of the NO_y predicted from the N_2O/NO_y relationship is gaseous HNO_3. *Kawa et al.* [1990] estimate that in the Arctic polar region, 50 to 80% of the measured NO_y is HNO_3.

From this relationship, saturation of HNO_3 with respect to NAT is expected at temperatures of 195 to 196 K for 5 ppmv of H_2O at 50 mbar and HNO_3 vapor pressure based on the observed values of NO_y^*. The heavy horizontal dashed curves in Figure 2 show the temperature of saturation of HNO_3 over NAT. When the measured temperature (the heavy solid line) drops below the horizontal dashed line, saturation is reached and NAT particle formation might be expected. Ice saturation would not be reached for these same environmental conditions until approximately 189 K. *Dye et al.* [1990*b*] reported that for the January 24 case there was evidence of some growth on the largest particles on the tail of the sulfate size distribution beginning at about 195 to 196 K (NO_y^*/HNO_3sat near 1) but that the large increase in volume did not begin until temperatures near 191 to 192 K (NO_y^*/HNO_3sat near 10) were reached. Similar features are seen for the other days as well.

To illustrate different particle spectra on different days and at different temperatures, we have plotted 300 s averages (60 km of flight path) of sequential size and volume distributions for each of the days with PSCs in Figures 6 and 7, respectively. The distributions are plotted in the $dN/d\log D$ form, where N is the concentration and D the diameter. In this form the area under any part of the curve is proportional to concentration (volume) of particles in that size interval. The first number in the upper right hand corner of each distribution gives the beginning time of the 300 s average, the second line the total concentration (Figure 6) or volume (Figure 7), and the last line the average temperature. The dashed line shows the lognormal fit to the Passive Cavity Aerosol Spectrometer number distribution for 891024 from 32000 to 33000 s discussed in Section 4.2. The parameters of this distribution are $N_o = 15$ cm^{-3}, modal diameter $D_g = 0.184$, $\sigma = 1.60$. The same curve is shown for each distribution on all days to demonstrate relative changes on each day and between days.

The first and second columns for each day show the sulfate particle distribution at about 205 and 200 K, respectively. The shape of the distributions for each of the days is quite similar except for 890130, which shows fewer and smaller particles than the other days. The plots in the third column show the observed distribution near 194 K, a temperature which is slightly less than the temperature at which saturation of HNO_3 over NAT occurs, while those in the fourth column are near 192 K and at greater supersaturations. On 890103 and 890112 the temperature did not drop to 192 K, so the fourth column shows the distribution at the coldest temperature observed on that day. The fifth column, labelled "I" shows a characteristic size distribution in the most prominent part of type I PSCs observed for each day. The column labelled "II" shows a distribution from regions containing the most and largest particles, which are thought to be type II particles. The last column shows a distribution for those days and times in which the ER-2 flew in a denitrified airmass (see below). Although most of the flight of 890130 was in denitrified air, the conditions were so disturbed that we have not shown a denitrified distribution for that day.

The first suggestion of NAT growth appears at NO_y^*/HNO_3sat ratios slightly greater than 1 (temperatures near 195 K) as the development of enhanced concentrations (a shoulder) on the larger particles of the sulfate distribution between 0.8 and 1 μm diameter. This can be seen in the 194 K column of Figures 6 and 7 for 890120, 890124, 890125, and 890130. Even though NAT saturation has been reached at this temperature for the distributions shown for 890103, 890116, and 890119 there is no discernible enhancement of the larger particles. For the distribution shown for 890112 there appears to be a deficit of the intermediate sized particles rather than an enhancement. The data suggest that the formation of NAT particles on the larger sulfate particles did not begin until later in the history of the vortex. As temperature decreases from 194 to 192 K this enhancement

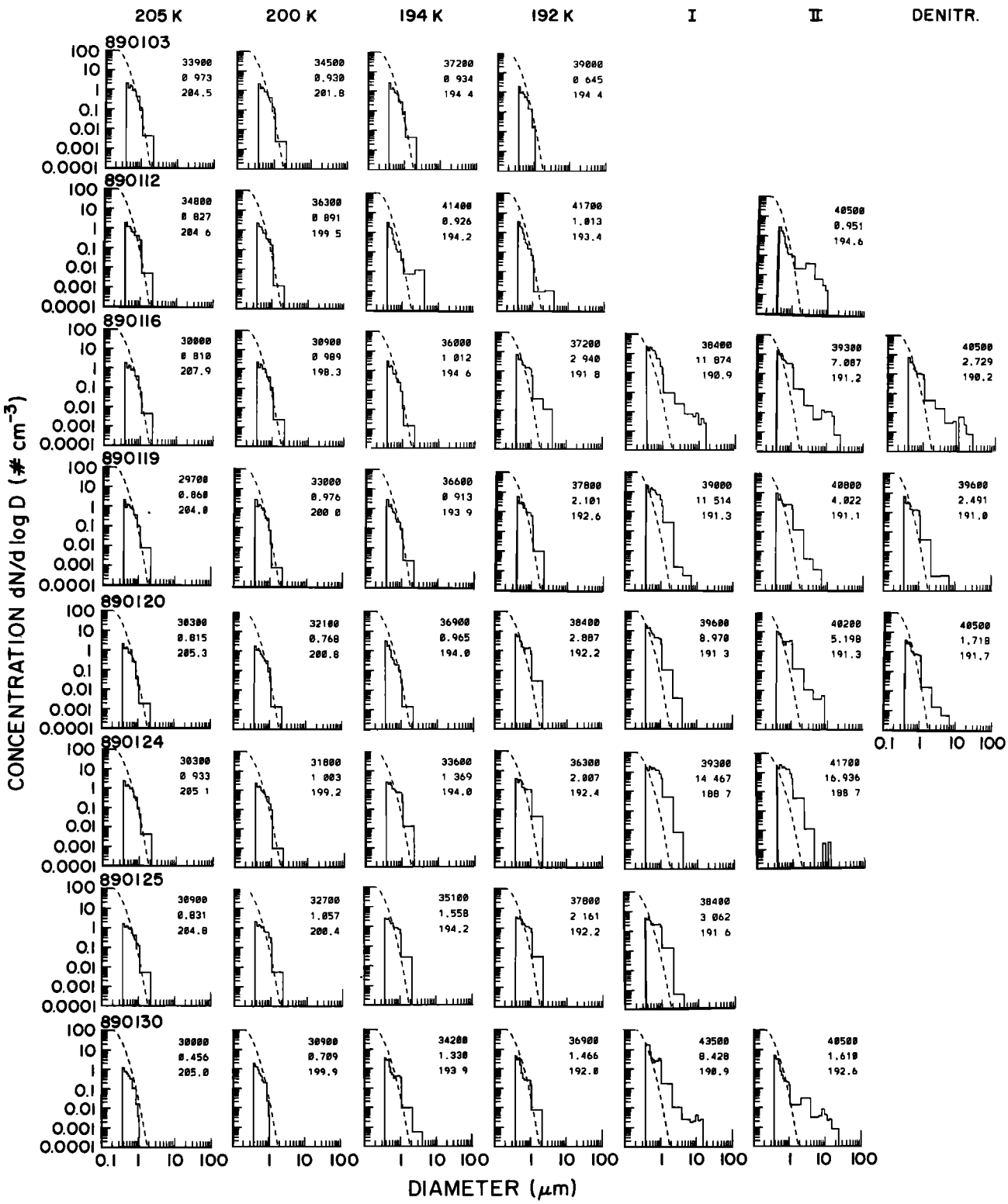

Fig. 6. The 300 s averages of FSSP 300 measurements illustrating particle size distributions for each day at different temperatures and in type I and type II PSCs and denitrified regions. The numbers in the upper right of each plot show the start time of each time period, the total concentration, and average ambient temperature, respectively. The dashed curve is a lognormal fit to the number distribution for 890124 from 32000 to 33000 UT (see text).

becomes more prominent. Even the 890116 and 890119 distributions are now showing an enhancement of particles near 1 μm.

The enhancement on the tail of the sulfate distribution is subtle, but we feel it is a physical feature of the observations not an instrumental artifact. *Hofmann et al.* [1990] also convincingly show a case where the 1 μm diameter particles begin to exceed the background concentration near NAT saturation, even though changes are not apparent in the profiles of the smaller particles. *Hofmann and Deshler*

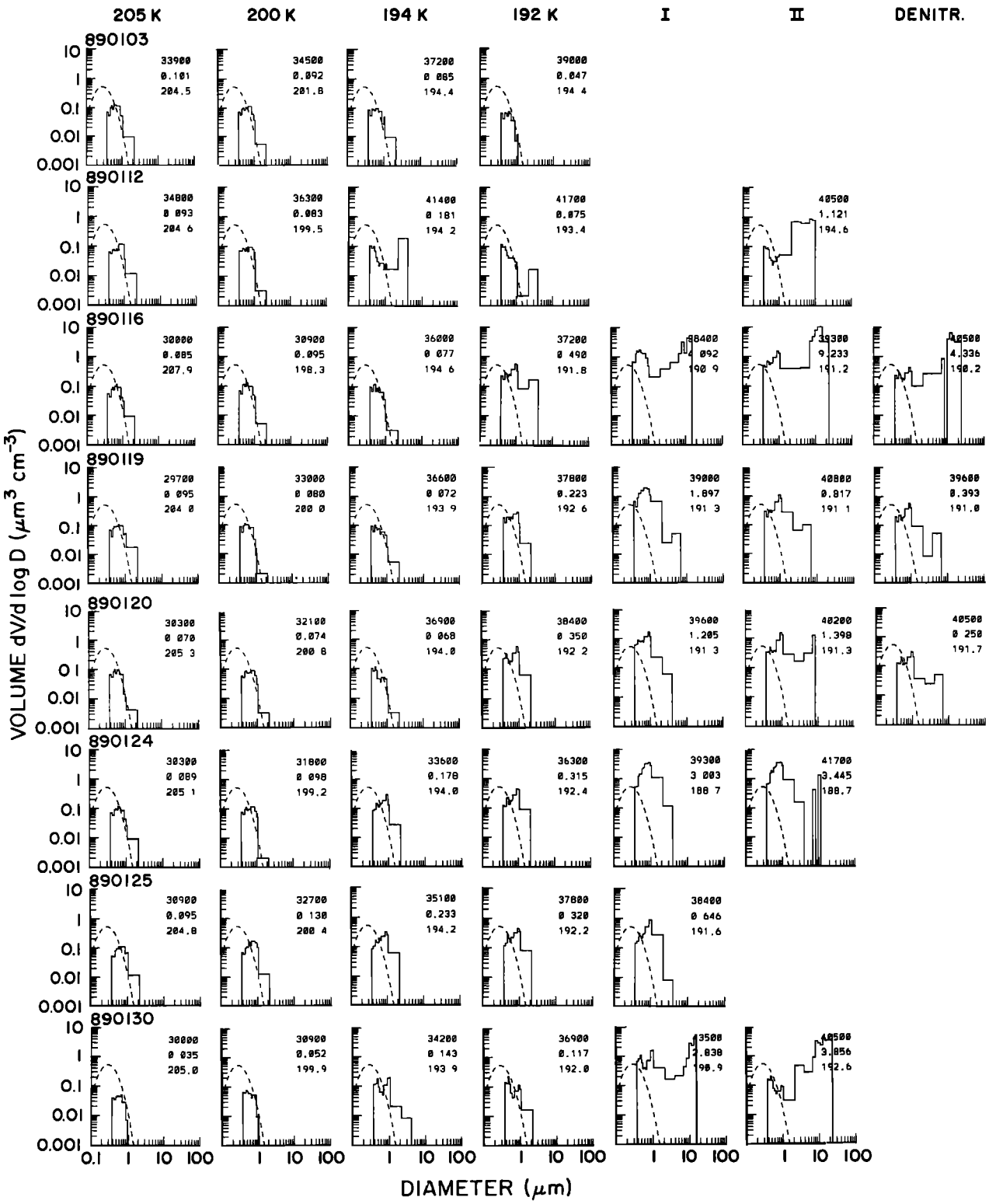

Fig. 7. Particle volume distributions for the same time periods shown in Figure 6.

[1990] also found in Antarctica that the largest particles in the sulfate layer seem to take part preferentially in NAT growth. Although it is within instrumental error, the NO_y comparisons with NO_y^* in Figure 7 of *Kawa et al.* [this issue] consistently hint at the presence of some NO_y in the aerosol at NO_y^*/HNO_3sat between 1 and 10.

Although a pronounced NAT cloud was not encountered on 890112, temperatures did drop below 195 K and briefly to nearly 193 K near 42000 s inside the vortex (Figure 2). The histograms at 194 and 192 K (41400 and 41700 UT s, respectively) show that 1 to 4 μm diameter particles were present at these coldest temperatures and the NO_y measurements

show some NO_y in the aerosol phase (see Figure 6 of *Kawa et al.* [this issue]). However, Figure 2 shows that just prior to 41400 sec UT, particles > 4 μm diameter were present and measurements from the microwave temperature profiler [*Gary*, 1989] show temperatures above the ER-2 reached the frostpoint suggesting that these large particles might have sedimented to the ER-2 altitude. The evidence suggests that either type I and/or type II particles might have been present, but the data are insufficient to determine if the 1 to 4 μm diameter particles were NAT.

4.5. *Main Occurrence of Type I Clouds*

In Figure 2 there are large regions in which saturation of HNO_3 with respect to NAT has occurred but with little evidence of significant particle growth. Likewise, the departure of the measured particle volume from sulfuric acid deliquescence in Figure 3 is relatively small until temperatures down to 193 K are reached. However, when the temperature decreases below 192 K (corresponding to large apparent saturation ratios), very large increases in volume occur. The observations suggest three separate regimes which we interpret as, first, the swelling of the sulfuric acid droplets as temperature decreases to 195 K and below; next, the activation and growth of a few NAT particles near saturation ratios slightly greater than 1 between 195 and about 193 K; and at colder temperatures the abrupt transition as the majority of the sulfate are activated to form NAT. In Figure 8 we see that the large increases in particle volume do not occur until apparent saturation ratios approach 10.

The major feature of the observations in Figures 3 and 8 is the large increases in volume (and concentration) which occur at temperatures of 192 to 193 K and apparent saturation ratios of 5 to 10 for each of the days. If the number of particles nucleated is determined primarily by cooling rate, we would not expect to see such consistency with temperature on different days, unless the cooling rate were the same on the different days. While this may be possible, it seems unlikely given the span of time with different meteorological conditions over which the PSC observations were made. Another possible explanation for this temperature dependence is that only a small fraction of the sulfuric acid droplets are frozen at temperatures of 195 to 193 K and only this small fraction act as nuclei for NAT shortly after HNO_3 saturation with respect to NAT is achieved in the airmass. The remaining droplets remain supercooled, until colder temperatures near 191 to 192 K are reached. At that point they freeze homogeneously, thus allowing most, if not all, of the H_2SO_4 particles to act as nuclei for NAT and create the main onset of the cloud which the FSSP observes.

In Figure 2 we see that increases in particle concentration are frequently anti-correlated with temperature. At temperatures less than 195 K, we believe the correspondence between temperature and particle concentrations, which is often most evident in the intermediate sized particles (0.6 to 4 μm), reflect the beginnings of NAT particle formation. For temperatures between 193 and 190 K there are often periods when decreases in temperature of a couple of degrees are associated with large increases in concentrations and volumes such as those for 890116 between 36000 and 41000 s, 890119 between 36600 and 37800 s, 890120 between 36000 and 38600 s and 890124 between 33000 and 37000 s. This is particularly true for the 0.6 to 4.0 μm particles. The excursions in temperature often have periodicities of 10 to 15 min corresponding to distances of 200 to 300 km and are probably a result of wave motion frequently seen in the Arctic data by the microwave temperature profiler [*Gary*, 1989].

4.6. *Type II Particles*

Saturation with respect to water ice was observed only on 890124 during the AASE. Thus, the information which we have on conditions in the region in which type II particles might have been nucleating and growing is very limited. *Gandrud et al.*, [1990] showed that the particles > 4 μm diameter observed on 890130 probably formed at higher altitudes and sedimented to the ER-2 altitude. There were four other flights, 890112, 890116, 890119, and 890120 during which the FSSP detected regions with particles > 4 μm diameter (Figure 2). On each of these days, measurements made by the microwave temperature profiler [*Gary*, 1989] show that temperatures 1 to 2 km above the aircraft reached the frostpoint in the locations in which large particles were observed. For example, measured temperatures for 890120 at pressure altitudes of 21, 22, and 23 km with the ER-2 at about 20 km are shown in Figure 9. The frostpoint temperatures for these altitudes, shown on the right side of Figure 9, are about 188.0, 187.2, 186.4 K, respectively, assuming that the 5 ppmv of water vapor measured at 20 km [*Kelly et al.*, 1990] also applies to the higher altitudes. From Figure 9 we see that the frostpoint was reached less than 1 km above the aircraft in the same region as that in which ice particles were observed. Additionally, there was a deep layer with temperatures colder than the frostpoint.

Sedimentation velocities for 4, 10, and 20 μm diameter particles with a density of 1 g cm^{-3} falling at 20 km altitude were calculated, following *Kasten* [1960], to be about 100, 400 and 1200 m per day, respectively. When they are falling in air subsaturated with respect to ice, some evaporation would be taking place. *Toon et al.* [1989] calculate that an evaporating ice particle of 20 μm diameter at 20 km could have originated as a particle > 100 μm one day earlier when falling in subsaturated air. *Wofsy et al.* [1990] also suggest that ice particles falling in a region where saturation of HNO_3 with respect to NAT occurs, might be coated by NAT and hence reduce the evaporation of water. Given the many hours or even days time scale of PSC events, it seems quite possible that all of the particles > 4 μm diameter which we observed can be explained on the basis of sedimentation of ice particles from above (or for 890124 formation in situ). The concentrations of type II particles which we observed and are lower limits were about 0.001 to 0.01 cm^{-3}, which is a factor of 100 to 1000 fewer than the NAT particles.

4.7. Particle Distributions in Regions of Denitrification

Measurements of NO_y presented in *Kawa et al.* [this issue] show that denitrification occurred on 890116, 890130, and very briefly on 890120. On 890119 and 890125, NO was measured in place of NO_y, and we cannot directly determine if denitrification was present. The ratio between the measured NO_y and NO_y^* provides a method for determining regions of denitrification and also enhancements of NO_y in the presence of PSCs. When NO_y is lost from the airmass, the ratio is < 1, whereas when NAT PSCs are present, NO_y is enhanced by the instrument and the ratio is > 1. See *Fahey et al.*, [1990] and *Kawa et al.* [this issue] for details. The NO_y/NO_y^* ratio is plotted in Figure 10 for days 890112,

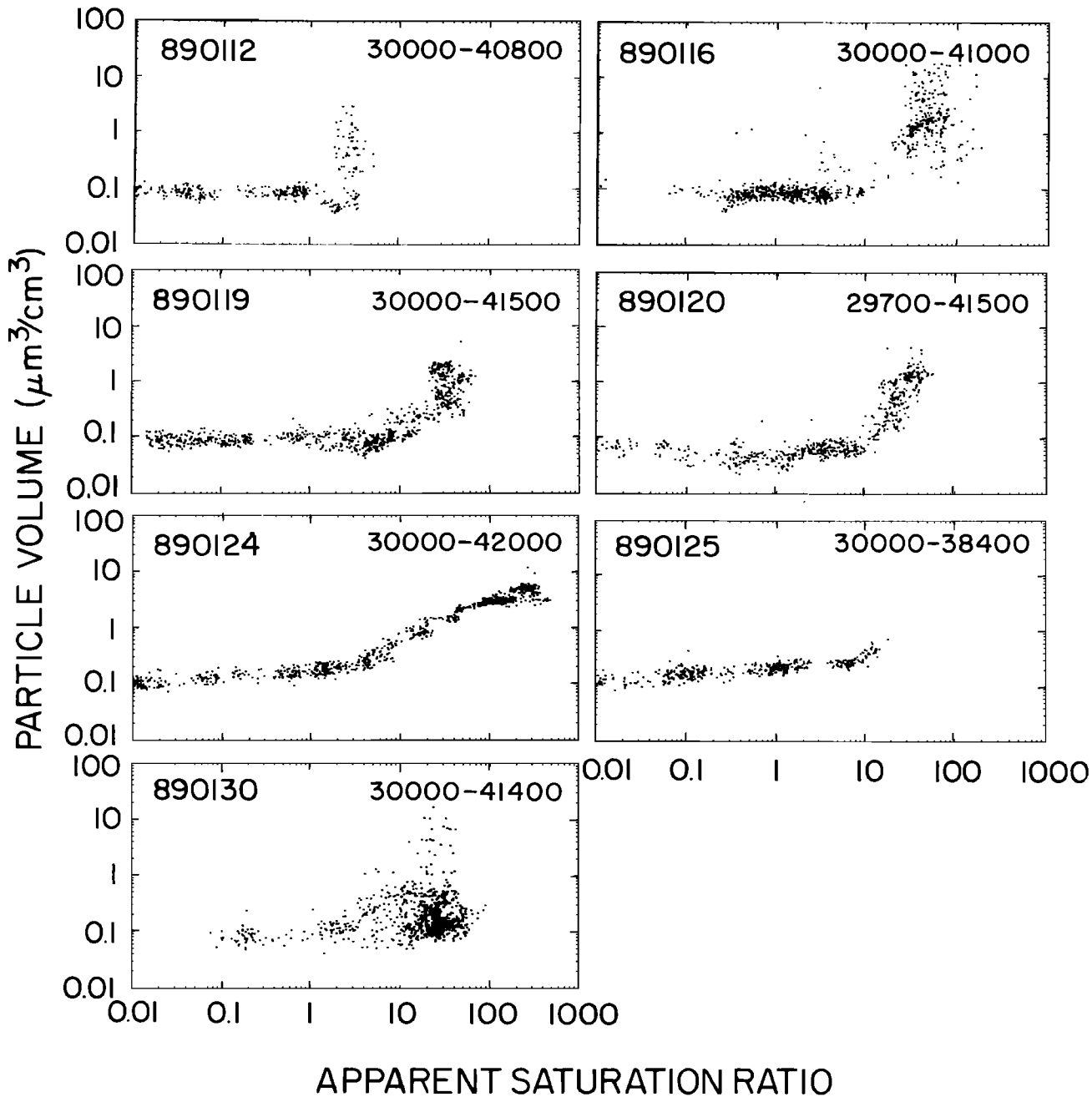

Fig. 8. Measured particle volume from the FSSP 300 plotted as a function of NO_y^*/HNO_3sat, the apparent saturation ratio of HNO_3 over NAT for the ER-2 flights in PSCs.

890116, and 890120. From comparison of particle concentrations in Figure 2 with NO_y in Figure 10 we see that the regions with ratios > 1 correspond well with times when large increases in particle concentrations occur. *Kawa et al.* [this issue] discuss these enhancements in more detail. Also note that for 890116 from about 40000 to 42000 s and 890120 briefly near 41000 s the ratios in Figure 10 are substantially less than 1, i.e. denitrification has occurred in this region. From comparison with Figure 2, we see that although the ambient temperature remained below 192 K, there are significant decreases in particle concentration in the same regions in which denitrification has occurred. This is illustrated more clearly in Figure 11 in an extended plot for 890116 and in the last column of Figures 6 and 7. Although particle concentrations in the PSCs decreased for both the smallest size category, 0.4 to 0.6 μm diameter and the intermediate size category, i.e., 0.6 to 4 μm diameter, the ratio between the intermediate and smallest sized particles is lowest in this region.

For both 890116 and 890120 the denitrified region was at the most northern part of the ER-2 flight path. Although NO_y was not measured on the 890119 flight, a decrease in particle concentration and volume also occurs on 890119 at the northernmost part of the ER-2 flight track. A comparison of NO_y^* with FSSP volume for 890119 and 890116 shows that on both days NO_y^* remains relatively constant in the

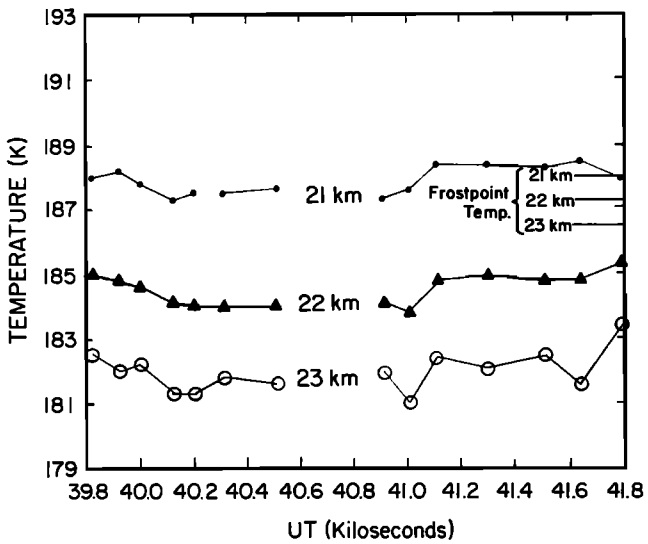

Fig. 9. Temperatures measured by the microwave temperature profiler above the flight track of the ER-2 on 890120. The frostpoint temperatures for each altitude are as indicated.

PSC regions, but there are big decreases in FSSP volume on both days. The evidence suggests that the northern part of the 890119 flight is also denitrified.

The lidar observations of *Browell et al.*, [1990] for the 890111 flight of the NASA DC-8 aircraft show that type Ia PSCs, which *Toon et al.* [1990] have inferred to be larger NAT particles, occurred deep in the vortex. This is the same region in which the FSSP measurements show decreases in particle concentration and volume, particularly for intermediate size particles on the tail of the sulfate distribution. This is supported further by the observations of sulfate aerosol by J. C. Wilson et al. (submitted manuscript, 1991), who also report that sulfate size distributions in denitrified regions show a reduction of particles on the large droplet tail of the distribution. Both the lidar and FSSP observations are consistent with the concept that denitrification can occur by activation, in some circumstances, of only a small fraction of the sulfate particles to form NAT particles which are large enough to then slowly sediment out of the airmass. Wind speeds deep in the vortex away from the polar jet are less and may result in slower cooling rates.

4.8. Summary of PSC Particle Characteristics

The measurements of concentration, surface area, and volume from the FSSP 300 are summarized in Table 2 for what we consider to be type I and type II particles. The concentrations for type I particles in the size range 0.4 to 4 μm were from about 2 to a maximum of 16 cm^{-3} for 890124. The lower limit is very approximate because we cannot distinguish small NAT particles from sulfate. If we presume that only those on the shoulder of the distribution, i.e., 0.6 to 4 μm were activated at temperatures between 195 and 193 K, the minimum concentration would be about 0.1 to 1 cm^{-3}. The concentration of type II particles observed ranged from 0.001 to 0.01 cm^{-3}. These are probably lower limits for the concentration of type II particles because the ER-2 did not get into the main body of type II clouds.

The volumes observed for type I particles ranged from about 0.5 to 5 μm^3 cm^{-3}. Again the lower limit is not well defined. The equivalent mass for NAT would be about 2 to 20 ppbv. As discussed by *Kawa et al.* [this issue] the larger values are larger than would be expected compared to the measured NO_y mixing ratios. For type II particles the range of observed volumes was 0.1 to 8 μm^3 cm^{-3} with the maximum on 890116. These volumes were calculated assuming spherical particles. Replicas of type II particles in the Antarctic have shown that they are not spherical, but are columnar in shape with axial ratios ranging from 2 to 3 [*Goodman et al.*, 1989]. Because the scattering from nonspherical particles is less than for spherical particles of equivalent volume diameter [*Zerull*, 1976], these volume estimates are probably underestimates. Some particles larger than those which can be sized with the FSSP 300 (> 24 μm diameter) may exist, also leading to an underestimate of volume.

The surface area for type I particles ranged from about 1 to as large as 20 μm^2 cm^{-3} for 890124 before H_2O saturation was reached. The replicas collected by *Pueschel et al.* [this issue] on 890116 and 890124 (the only two days with replicas) were circular, implying that the NAT particles seen on this day were spherical or nearly spherical and did not have a lot of irregularities and hence additional surface area. Thus, the measurements of surface area of NAT particles from the FSSP 300 should be reasonably accurate for use in heterogeneous reaction calculations. Assuming spherical particles, the surface area of the type II particles ranged from 0.1 to 3 μm^2 cm^{-3}. As discussed earlier, these particles were probably not spherical, some larger particles were probably missed, and the ER-2 did not enter the core of any type II clouds, all of which give underestimates of type II surface area.

The concentrations shown in Table 2 for the type I particles are larger than the concentrations of condensation nuclei (CN) measured by the CN counter [*Wilson et al.*, 1990] by a factor of 2 to 3 as was previously pointed out by *Dye et al.*, [1990*b*] for the 890124 case. They are also larger than the sulfate concentrations for 890124 determined from impactor wires by *Pueschel et al.* [this issue] by a factor of 3 to 4. *Hofmann et al.* [1990] present CN and particle measurements which show agreement between the CN and the number of NAT particles apparently activated. Because of the disagreement between the FSSP measurements and those of

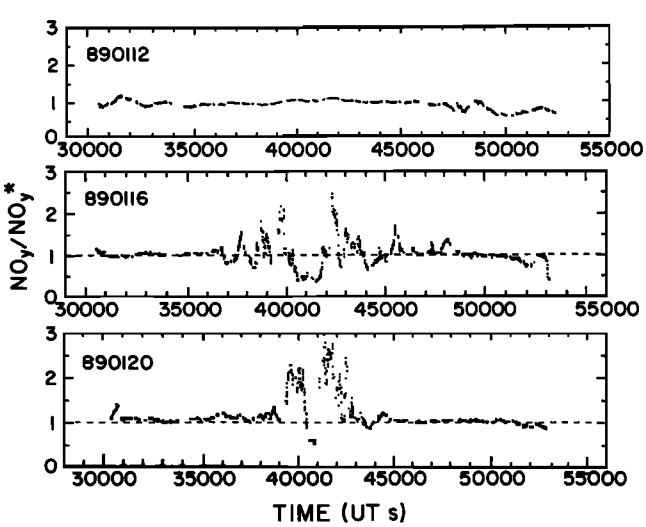

Fig. 10. The ratio of NO_y to NO_y^* versus time for 890112, 890116, and 890120 (see text).

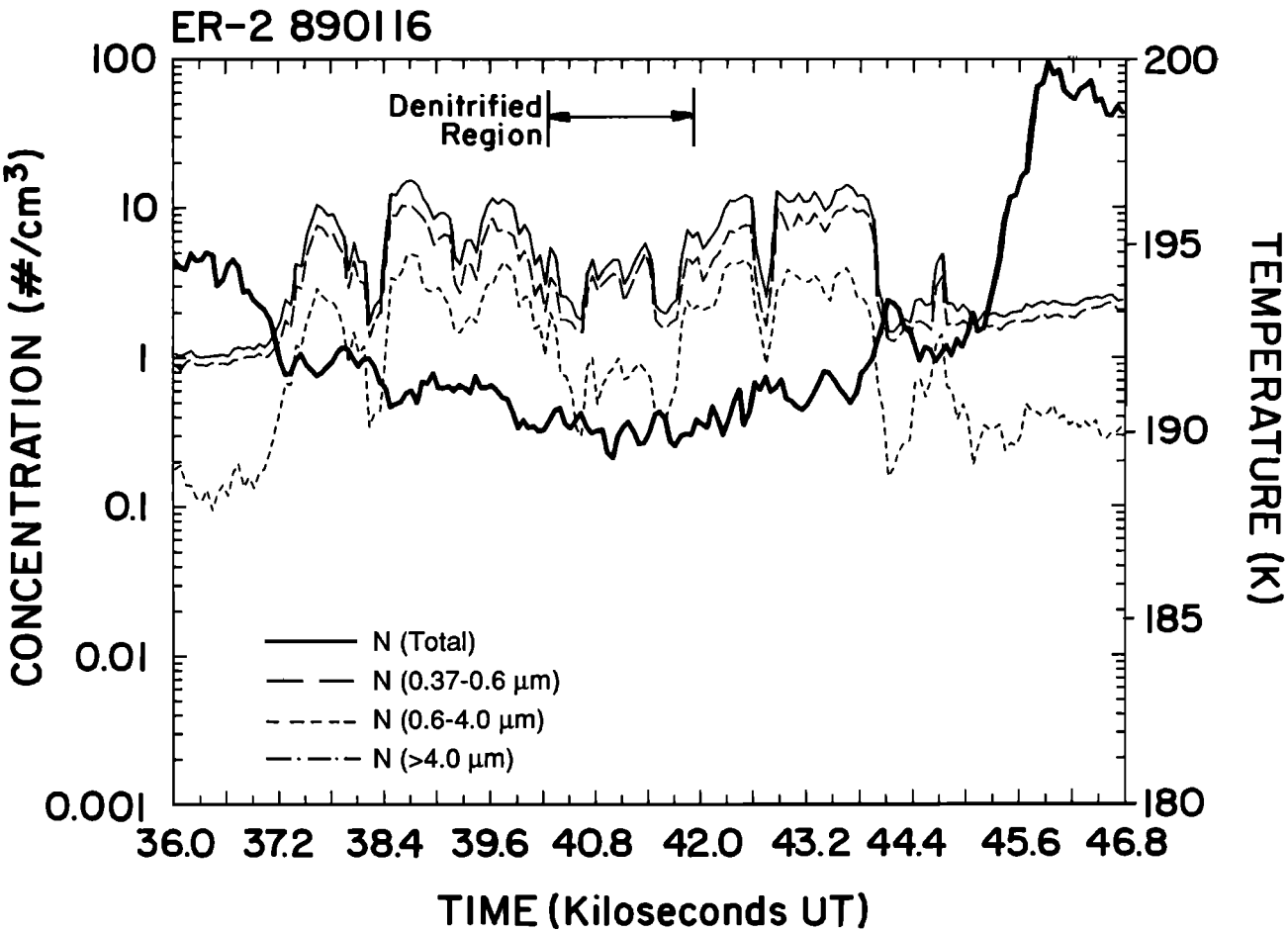

Fig. 11. An expanded plot for 890116 similar to those in Figure 2 to illustrate changes in particle concentrations and sizes in the denitrified region

others, we have carefully investigated [*Baumgardner et al.*, this issue] all avenues we can think of, including recent laboratory tests of electronics at very cold temperatures, which might lead to an error in sample area determination or a shift in sample area at the cold temperatures encountered in the stratosphere. We have found no evidence from these or earlier tests to suggest that the sample area is different than the 0.05 +/- 20 % mm^2 previously quoted. One reviewer suggested that the noise in the first channel of the FSSP might be the source of the large concentrations, but if we disregard the first channel entirely the concentrations in PSCs are reduced by only 1 to 2 cm^{-3}.

We are left with an unresolved problem: the concentrations of NAT particles measured with the FSSP in well developed PSCs are larger than the CN concentrations measured outside of PSCs and larger than the concentrations suggested by impactor wires or the PCAS in the overlap region where all three instruments make measurements (J. C. Wilson et al., submitted manuscript, 1991). Is it possible that particles smaller than the lower limit of the CN counter (0.02 μm diameter) were activated to form NAT particles, or is it simply instrument problems? Additional field and laboratory studies are necessary before this issue can be resolved.

TABLE 2. Summary of PSC Particle Characteristics

	Type I	Type II
Concentration, cm^{-3}	~2 to 16	0.001 to 0.01
Volume, μm^2 cm^{-3}	~0.5 to 5	0.1 to 8
Surface area, μm^2 cm^{-3}	~1 to 20	0.1 to 3

Although there is some variability in the observed size distributions for NAT particles, the size and volume distributions in Figures 6 and 7 show a preferred volume mode for NAT particle formation between 0.6 and 1 μm diameter, a drop beyond 1 μm, and very little volume out as far as 4 μm diameter. The appearance of this mode at that size suggests that it is indeed the tail of the sulfate distribution which is being preferentially activated to form NAT particles, particularly those at lower saturation ratios of HNO_3 with respect to NAT. There are clearly times however, when the major fraction, if not all, of the sulfate particles appear to have been activated to form a monomodal spectrum (see column I of Figures 6 and 7). However, the size distributions which are likely to contain primarily NAT particles (based on temperatures 192 K or less) do show considerable variation with some being monomodal as mentioned above and others having a main number mode near 0.5 μm diameter and a shoulder near 1 μm. These variations suggest that different cooling rates do influence the number of NAT particles nucleated as suggested by a number of investiga-

tors and by the modeling studies of *Poole et al.* [1990] and *Wofsy et al.* [1990]. This might also be the effect of some parcels having experienced greater temperature fluctuations than others.

The observations of *Hofmann et al.* [1989*a*, *b*, 1990] and *Hofmann and Deshler* [1989] in the Arctic have shown features similar to the distributions we show. They report that the majority of the sulfate particles have been nucleated to form NAT with distributions showing a small number mode near 0.4 μm diameter and another mode at about 4 μm diameter. They suggest that larger particles were nucleated from larger, frozen sulfate particles and the smaller ones might have formed from condensation of HNO_3 onto supercooled liquid sulfate particles to form ternary mixtures. The small mode is similar to many of the distributions we found, for example the early phases of the 890119, 890120, and 890124 clouds and the 890125 and 890130 clouds. They report observations made in the 890130 cloud above Kiruna Sweden, which is to the west of the ER–2 flight track. Their distributions look similar to ours for that day in that they report most of the particles near 0.4 μm with a larger mode near a few microns diameter. One general difference between their reported distributions and ours is for the larger sizes. The FSSP 300 shows very few particles extending beyond 1 μm diameter. By comparison, in Antarctica they frequently report particles of a few microns in size which they infer to be NAT. As discussed above, when we have observed particles larger than 4 μm in the Arctic, temperatures above the ER–2 altitude reached the frostpoint and it seems likely that the largest particles (and perhaps even 4 to 5 μm diameter particles) sedimented to the aircraft altitude. We have found no clear evidence for NAT particles as large as 4 μm diameter during the ER–2 flights.

We must be careful in drawing conclusions from comparisons of this nature. The measurements were made at different times and locations and, except for 890130, in different clouds. Information on the upwind characteristics of the air mass is lacking, as is the detailed previous temperature history of the air parcel in and upwind of the cloud, and other factors which determine the nucleation of the particles. This kind of information is absolutely essential if we are to understand the mechanisms of the nucleation and growth of PSC particles. Measurements need to be made from the leading edge of the cloud along the airmass trajectory and improved aerosol instrumentation is necessary including the ability to determine composition of the particles.

5. Cooling Rate and Sulfate Freezing

Previous studies [e.g. *Poole et al.*, 1990; *Wofsy et al.*, 1990] have assumed that the sulfuric acid droplets will all be frozen at temperatures warmer than those at which NAT condensation could begin and therefore have concluded that cooling rate along with free energy barrier was the dominating influence which controlled the number of particles which could be nucleated. In this paper we have presented evidence that the majority of the sulfuric acid droplets remain liquid to temperatures < 193 K and argue that homogeneous freezing may not occur until temperature has decreased further, perhaps as low as 190 K, where the remaining droplets would freeze.

For heterogeneous freezing, i.e., nucleation from a foreign body in the liquid, the probability of freezing is dependent upon droplet size (see Pruppacher and Klett, for example), the larger the volume, the greater the probability. Thus, before homogeneous freezing occurs, the droplets on the tail of the sulfate distribution would have a higher probability of being frozen than those at smaller sizes and therefore a higher probability of acting as nuclei for NAT formation. If this is correct, when an air parcel first reaches a temperature at which NAT condensation could occur (196 to 195 K at 20 km in the Arctic) only a fraction of the sulfate aerosols can readily act as nuclei for NAT. But as the temperature cools further and homogeneous freezing of the sulfuric acid droplets has occurred, all of the sulfate are available as nucleation sites for NAT.

We suggest the following scenario as a conceptual model of the roles of cooling rate and homogeneous nucleation of sulfuric acid droplets in the formation of polar stratospheric cloud particles. As with any conceptual model it needs to be tested by further observations and model simulations, but it seems to fit observations, both ours and others in the literature.

The first particles to nucleate and grow are from the tail of the sulfate distribution, as observed herein for the 890120, 890124, and 890125 cases. If the cooling rate is rapid, the rate at which HNO_3 becomes available for NAT growth is rapid. Hence, the small number of growing NAT particles cannot deplete the supply of HNO_3 and large supersaturations of HNO_3 with respect to NAT develop. As the parcel cools past the temperature necessary for homogeneous freezing, all sulfuric acid droplets freeze and because of the very high supersaturations, rapidly nucleate to form NAT particles. The available HNO_3 is distributed among many particles with the result that the NAT particles are small and have one dominant mode, as observed for all days with type I PSCs except 890130 (see column I of Figures 6 and 7). An alternative to this explanation is the suggestion of *Hofmann and Deshler* [1990] that for fast cooling rates, the many smaller NAT particles are formed from the condensation of HNO_3 and H_2O onto supercooled liquid sulfate particles. However, the impactor results of *Pueschel et al.* [this issue] in the fast cooling rate PSC of 890124 suggest that the nitric acid containing particles were solid, thus refuting this hypothesis.

When the cooling rate is slow, the first NAT particles can begin to form on the fraction of sulfate particles which are already frozen after saturation of HNO_3 with respect to NAT occurs. There is a higher probability of the larger sulfate particles being frozen, but even if a fraction of the smaller ones are frozen and nucleate NAT particles, the small ones will grow more rapidly than the larger NAT particles and, if growth proceeds sufficiently long, have a tendency to produce relatively uniform sized particles. This convergence toward uniform sizes is typical of a condensational growth process [e.g., *Pruppacher and Klett*, 1978]. The resulting size will be a function of the number of NAT particles which are growing, the amount of HNO_3 available for condensation and, if equilibrium is not reached, the amount of time available for growth. Because H_2O is abundant it will not be a limiting factor. As the temperature decreases, HNO_3 will condense out of the airmass. When the particles have cooled to 192 K the saturation mixing ratio of HNO_3 with respect to NAT will have decreased to 0.4 ppbv [*Hanson and Mauersberger*, 1988]. Thus, by the time temperatures are sufficiently cold to homogeneously nucleate the unfrozen sul-

furic acid droplets, the gaseous HNO_3 could be potentially reduced to mixing ratios of 0.4 ppbv or less by deposition on growing NAT particles. Consequently, there would be much less growth on the smaller, homogeneously nucleated sulfate particles. Because of the lower population of the select few which grew earlier, the resulting NAT particles will be larger and their size will depend upon, among other things, the fraction of sulfate particles previously frozen. This fraction might increase as the winter progresses. From the FSSP 300 observation for 890120, 890124 and 890125 we estimate that about 0.1 to 1% of the total sulfate concentration might be involved in this early stage of NAT formation. We do not have direct observations of large NAT particles from our data, only the indirect evidence in the denitrified regions. However, *Hofmann and Deshler* [1991] report such observations from Antarctica. Also, the lidar observations of type Ia particles deep in the vortex by *Browell et al.* [1990] support this idea. We wonder if cooling rates might often be less deep in the vortex, because of weaker horizontal winds away from the polar jet. If so, it might be a preferential place for large NAT particle formation and denitrification.

If the lack of frozen sulfate particles does limit the number of nuclei available for NAT formation, it can happen only once in a given air parcel in the vortex. Once the H_2SO_4 droplets are frozen, they will remain solid. However, it may take considerable time for all of the droplets in the vortex to freeze, i.e. for the entire airmass to have cooled below the needed temperature, approximately 190 K depending upon H_2O mixing ratios.

When all of the sulfuric acid droplets are frozen by previous exposure to temperatures colder than that necessary for homogeneous freezing, as would be expected in the Antarctic vortex late in the austral winter, all of the sulfate particles can act as nucleation centers for NAT growth. The formation of NAT could appear at saturation ratios of HNO_3 with respect to NAT only slightly in excess of one as was observed by *Fahey et al.*, [1989] on August 17, 1987 (Figure 12) and in other events in the Antarctic. It is interesting to note that *Crutzen et al.* [1988] anticipated that a difference might exist between the Arctic and Antarctic based on the assumption that the sulfuric acid droplets must be frozen before NAT particles could be nucleated, and the knowledge that air masses in Antarctica frequently experience temperatures colder than 190 K but temperatures this low are less frequent in the Arctic.

The August 17, 1987, PSC observations of *Fahey et al.* [1989], where NAT clouds did form near saturation ratios of 1, were in a "minihole" in which stratospheric air was being lifted over a tropospheric ridge leading to rapid adiabatic

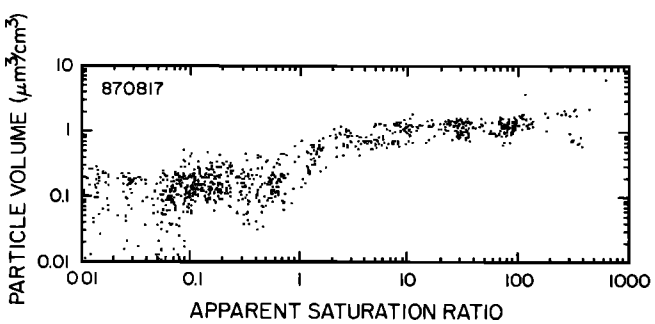

Fig. 12. As in Figure 8 except for data collected in Antarctica on 870817.

cooling rates [*McKenna et al.*, 1989]. Total PSC particle concentrations in this event were 4 to 5 cm^{-3} with a volume mode between 1 to 2 μm diameter. The concentrations and sizes of this event are similar to those which we have found in the Arctic, where cooling rates were also high. We believe it is difficult to explain, for these two cases, the similarities in size distribution, but differences in the apparent saturation ratio at which PSCs occur with arguments of cooling rate alone. To us the effects of homogeneous freezing of liquid H_2SO_4 droplets in the Arctic seems a more likely explanation.

If the above scenario is correct, it could explain (1) the first appearance of NAT on the tail of the sulfuric acid distribution at saturation ratios only slightly larger than one; (2) the consistency with temperature of the rapid onset of the main cloud observed herein, and by *Hofmann et al.* [1990], at a temperature near 191 to 192 K, which we infer to be near the temperature at which homogeneous freezing occurs; (3) the observation that sometimes there is a large particle mode of a few microns diameter [*Hofmann et al.*, 1988; *Hofmann and Deshler*, 1991] which apparently grew from the large particle portion of the sulfate distribution; (4) the difference in apparent saturation ratio at the main occurrence of PSCs in these observations (saturation ratios $\sim$10) and the one of *Fahey et al.* [1989] in Antarctica (saturation ratios $\sim$1).

Because of the strong temperature dependence of the saturation vapor pressure of HNO_3 over NAT, it is difficult to unambiguously separate the effect of cooling rate and hence energy barriers from homogeneous freezing of H_2SO_4 droplets. However, our observations do show an increase in the sulfuric acid volume measured with the FSSP 300 as temperature decreases from 210 to $<$ 193 K, and this is expected from deliquescence. This, in itself, suggests that homogeneous freezing of the sulfuric acid droplets occurs somewhere in the cooling cycle and may be playing a role in the formation of NAT. Additional model simulations are necessary to elucidate the roles that may be played by cooling from large scale lifting or wave motions which alter the recent temperature history of the air parcel and homogeneous freezing of the sulfate. Laboratory studies of the supercooling and nucleation of sulfuric acid and the nucleation and transition to nitric acid condensation are also important, including measurements of the refractive index and density of the H_2SO_4 hydrates and NAT. It is extremely important to have measurements made in a Lagrangian framework along the trajectory of different air masses. The lack of airborne instruments capable of measuring the entire spectrum of sulfate and NAT particle sizes with good size resolution without volatilization and the inability to measure particle composition directly are serious impediments to progress. Cooling rate is an important observational aspect which, for the most part, has not been quantitatively included in discussions of particle measurements. In particular, temperature fluctuations resulting from deviations of air parcels from idealized synoptic scale motions need to be studied. The observations of *Gary* [1989] suggest that we should be thinking in terms of recent percent of time spent at temperatures colder than a certain value rather than cooling rate.

6. Conclusions

We have presented the size and volume distribution measurements from the FSSP 300 during the AASE and have

used them to examine cloud microphysical processes which are occurring in the winter polar stratosphere. We draw the following conclusions from the measurements:

1. Sulfuric acid solution droplets in the stratosphere remain liquid and grow by deliquescence during cooling to temperatures at least as low as 193 K. Arguments are made to suggest that homogeneous freezing of the sulfuric acid droplets might occur near 190 K in the Arctic.

2. Observations suggest that only a fraction of the sulfuric acid droplets are frozen when saturation of HNO_3 over NAT occurs and NAT particles could first begin to form. We speculate that the rapid increase in particle volume observed by the FSSP 300 which occurs at temperatures colder than 192 K, may be the result of the homogeneous freezing of H_2SO_4 droplets which can then act as nuclei for NAT formation.

3. The first indication of NAT particle appearance occurs for saturation ratios of HNO_3 with respect to NAT near 1 as an enhancement near 1 μm diameter on the large particle tail of the sulfate distribution. However, there are large regions in the Arctic in which NAT saturation has been reached, but in which significant formation of NAT particles has not occurred. The growth of NAT particles at supersaturations near one was not apparent during the first few flights of the project, but was seen for the last four flights with PSCs.

4. The main increase of particle volume indicative of type I clouds was encountered when the temperature decreased below 192 K and the apparent saturation ratio of HNO_3 with respect to NAT reached 10 or greater. This is in contrast with observations of *Fahey et al.* [1989] in the Antarctic where the main onset was found to occur near a saturation ratio of 1.

5. In the northernmost parts of some flights where denitrification was observed, particle concentrations decreased, particularly the upper tail of the sulfate distribution. This was the same region in which the lidar observations of *Browell et al.*, [1990] detected type Ia particles. The combined evidence supports the hypothesis that activation of a few NAT particles allows that fraction to grow larger and fall out of the airmass.

6. The variation in the shape of the NAT particle size distributions circumstantially supports the notion that cooling rate and past air parcel temperature history influence the number of NAT particles which are nucleated.

Acknowledgments. We would like to thank Joanne Parrish, Laurel Sanford, Duane Allen, and Keith Barr for the collection, processing, or analysis of the data; David Fahey, Chuck Wilson, and Rudolph Pueschel for stimulating discussions in all aspects of this work; Graham Feingold for help with the truncated lognormal distribution; and Brad Baker, Charles Knight, and Stephan Bormann for comments on the manuscript. This work was partially supported by the NASA Upper Atmospheric Research Program. The National Center for Atmospheric Research is funded by the National Science Foundation.

REFERENCES

Arnold, F., H. Schlager, J. Hoffmann, P. Metzinger and S. Spreng, Evidence for stratospheric nitric acid condensation from balloon and rocket measurements in the Arctic, *Nature*, *342*, 493–497, 1989.

Baumgardner, D., J. E. Dye, and B. W. Gandrud, Calibration of the FSSP used on the ER-2 during the AAOE, *J. Geophys Res.*, *94*, 16,475–16,481, 1989.

Baumgardner, D., J. E. Dye, R. G. Knollenberg and B. W. Gandrud, Interpretation of measurements made by the forward scattering spectrometer probe (FSSP–300) during the Airborne Arctic Stratospheric Expedition, *J. Geophys. Res.*, this issue.

Browell, E. V., C. F. Butler, S. Ismail, P. A. Robinette, A. F. Carter, N. S. Higdon, O. B. Toon, M. R. Schoeberl, and A. F. Tuck, Airborne lidar observations in the wintertime arctic stratosphere: Polar stratospheric clouds, *Geophys. Res. Lett.*, *17*, 385–388, 1990.

Crutzen, P. J., and F. Arnold, Nitric acid cloud formation in the cold Antarctic stratosphere: A major cause for the springtime "ozone hole". *Nature*, *324*, 651–655, 1986.

Crutzen, P. J., C. Bruhl, U. Schmailzl, and F. Arnold, Nitric acid haze formation in the lower stratosphere: A major contributing factor to the development of the Antarctic "ozone hole", in *Aerosols and Climate*, edited by P. V. Hobbs and M. P. McCormick, pp., 287–304, A. Deepak, Hampton, Va., 1988.

Dye, J. E., B. W. Gandrud, D. Baumgardner, and L. Sanford, A survey of particle measurements in the Arctic from the Forward Scattering Spectrometer Probe Model 300, *Geophys. Res. Lett.*, *17*, 409–412, 1990*a*.

Dye, J. E., B. W. Gandrud, D. Baumgardner, K. R. Chan, G. V. Ferry, M. Loewenstein, K. K. Kelly, and J. C. Wilson, Observed particle evolution in the polar stratospheric cloud of January 24, 1989, *Geophys.. Res. Lett.*, *17*, 413–416, 1990*b*.

Fahey, D. W., K. K. Kelly, G. V. Ferry, L. R. Poole, J. C. Wilson, D. M. Murphy, M. Loewenstein, and K. R. Chan, In situ measurements of total reactive nitrogen, total water, and aerosol in a polar stratospheric cloud in the Antarctic, *J. Geophys, Res.*, *94*, 11,299–11,316, 1989.

Fahey, D. W., K. K. Kelly, S. R. Kawa, A. F. Tuck, M. Loewenstein, K. R. Chan, and L. E. Heidt, Observations of denitrification and dehydration in the winter polar stratospheres, *Nature*, *344*, 321–324, 1990.

Feingold, G., and Z. Levin, The lognormal fit to raindrop spectra from frontal convective clouds in Israel, *J. Clim. Appl. Meteorol.*, *25*, 1346–1363, 1986.

Gable, C. M., H. F. Betz, and S. H. Maron, Phase equilibria of the system sulfur trioxide–water, *J. Am. Chem. Soc.*, *72*, 1445–1448, 1950.

Gandrud, B. W., P. D. Sperry, L. Sanford, K. K. Kelly, G. V. Ferry, and K. R. Chan, Filter measurement results from the Airborne Antarctic Ozone Experiment, *J. Geophys. Res.*, *94*, 11,285–11,299, 1989.

Gandrud, B. W., J. E. Dye, D. Baumgardner, G. V. Ferry, M. Loewenstein, K. R. Chan, L. Sanford, B. L. Gary, and K. K. Kelly, The January 30, 1989 Arctic polar stratospheric cloud: Evidence for a mechanism of dehydration, *Geophys. Res. Lett.*, *17*, 457–460, 1990.

Gary, B. L., Observational results using the microwave temperature profiler during the Airborne Antarctic Ozone Experiment, *J. Geophys. Res.*, *94*, 11,223–11,232, 1989.

Goodman, J., O. B. Toon, R. F. Pueschel, and K. G. Snetsinger, Antarctic stratospheric ice crystals, *J. Geophys. Res.*, *94*, 16,449–16,457, 1989.

Hallett, J., and R. E. J. Lewis, Mother-of-pearl clouds, *Weather*, *22* 56–65, 1967.

Hamill, P. and L. R. McMaster (Eds.), Polar stratospheric clouds, NASA Conf. Public. 2318, 72 pp., 1984.

Hamill, P., O. B. Toon, and R. P. Turco, Characteristics of polar stratospheric clouds during the formation of the antarctic ozone hole, *Geophys. Res. Lett.*, *13*, 1288–1291, 1986.

Hanson, D., The vapor pressures of supercooled HNO_3/H_2O solutions, *Geophys. Res. Lett.*, *17*, 421–424, 1990.

Hanson, D., and K. Mauersberger, Laboratory studies of the nitric acid trihydrate: Implication for Antarctic ozone depletion, *Geophys. Res. Lett.*, *15*, 855–858, 1988.

Hofmann, D. J., and T. L. Deshler, Comparison of stratospheric clouds in the Antarctic and the Arctic, *Geophys. Res. Lett.*, *16*, 1429–1432, 1989.

Hofmann, D. J., and T. Deshler, Balloonborne measurements of polar stratospheric clouds and ozone at -93 C in the Arctic in February 1990, *Geophys. Res. Lett.*, *17*, 2185–2188, 1990.

Hofmann, D. J., and T. Deshler, Stratospheric cloud observations during formation of the Antarctic ozone hole in 1989, *J. Geophys. Res.*, *96*, 2897-2912, 1991.

Hofmann, D. J., J. M. Rosen, and J. W. Harder, Aerosol measurements in the winter/spring antarctic stratosphere, 1. Correlative measurements with ozone, *J. Geophys. Res.*, *93*, 665–676, 1988.

Hofmann, D. J., J. M. Rosen, J. W. Harder, and J. V. Hereford, Balloon borne measurements of aerosol, condensation nuclei, and cloud particles in the stratosphere at McMurdo Station, Antarctica during spring 1987, *J. Geophys. Res.*, *94*, 11,253–11,270, 1989*a*.

Hofmann, D. J., T. L. Deshler, P. Aimedieu, W. A. Matthew, P. V. Johnston, Y. Kondo, W. R. Sheldon, G. J. Byrne, and J. R. Benbrook, Stratospheric clouds and ozone depletion in the Arctic during January 1989, *Nature*, *340*, 117–121, 1989*b*.

Hofmann, D. J., T. Deshler, F. Arnold, and H. Schlager, Balloon observations of nitric acid aerosol formation in the Arctic stratosphere, II, Aerosol, *Geophys. Res. Lett.*, *17*, 1,279–1,282, 1990.

Jones, R. L., S. Solomon, D. S. McKenna, L. R. Poole, W. H. Brune, D. W. Toohey, J. G. Anderson, and D. W. Fahey, The polar stratospheric cloud event of January 24, Part 2, Photochemistry, *Geophys. Res. Lett.*, *17*, 541–545, 1990.

Kasten, F., Falling speed of aerosol particles, *J. Appl. Meteorol.*, *7*, 944–947, 1960.

Kawa, S. R., D. W. Fahey, L. C. Anderson, M. Loewenstein, and K. R. Chan, Measurements of total reactive nitrogen during the Airborne Arctic Stratospheric Expedition, *Geophys. Res. Lett.*, *17*, 537–540, 1990.

Kawa, S. R., D. W. Fahey, K. K. Kelly, J. E. Dye, D. Baumgardner, B. W. Gandrud, M. Loewenstein, G. V. Ferry, and K. R. Chan, The Arctic polar stratosphere cloud aerosol: Measurements of reactive nitrogen, total water and particles, *J. Geophys. Res.*, this issue.

Kelly, K. K., A. F. Tuck, L. E. Heidt, M. Loewenstein, J. R. Podolske, S. E. Strahan, and J. F. Vedder, A comparison of ER-2 measurements of stratospheric water vapor between the 1987 antarctic and 1989 arctic airborne missions, *Geophys. Res. Lett.*, *17*, 465–469, 1990.

Loewenstein, M., J. R. Podolske, K. R. Chan, and S. E. Strahan, N_2O as a dynamical tracer in the arctic vortex, *Geophys. Res. Lett.*, *17*, 477–480, 1990.

McCormick, M. P., H. M. Steele, P. Hamill, W. P. Chu, and T. J. Swissler, Polar stratospheric cloud sightings by SAM II, *J. Atmos. Sci.*, *39*, 1387–1397, 1982.

McElroy, M. V., R. J. Salawitch, S. C. Wofsy, and J. A. Logan, Reductions of Antarctic ozone due to synergistic interactions of chlorine and bromine, *Nature*, *321*, 759–762, 1986.

McKenna, D. S., R. L. Jones, J. Austin, E. V. Browell, M. P. McCormick, A. J. Krueger, and A. F. Tuck, Diagnostic studies of the Antarctic vortex during the 1987 Airborne Antarctic Ozone Experiment: Ozone miniholes, *J. Geophys. Res.*, *94*, 11,641–11,668, 1989.

Peter, Th., C. Bruhl, and P. J. Crutzen, Increase in the PSC formation probability caused by high flying aircraft, *Geophys. Res. Lett.*, *18*, 1465–1468, 1991.

Poole, L. R., and M. P. McCormick, Airborne lidar observations of Arctic polar stratospheric clouds: Indications of two distinct growth stages, *Geophys. Res. Lett.*, *15*, 21–23, 1988*a*.

Poole, L. R., and M. P. McCormick, Polar stratospheric clouds and the Antarctic ozone hole, *J. Geophys. Res.*, *93*, 8423–8430 1988*b*.

Poole, L. R., S. Solomon, B. W. Gandrud, K. A. Powell, J. E. Dye, R. L. Jones, and D. S. McKenna, The polar stratospheric cloud of January 24, 1989, Part 1, Microphysics, *Geophys. Res. Lett.*, *17*, 537–540, 1990.

Pruppacher, H. and J. D. Klett, *Microphysics of Clouds and Precipitation*, pp. 1–714, Reidel, Bingham, Mass., 1978.

Pueschel, R. F., K. G. Snetsinger, J. K. Goodman, O. B. Toon, G. V. Ferry, V. R. Oberbeck, J. M. Livingston, S. Verma, W. Fong, W. L. Starr, and K. R. Chan, Condensed nitrate sulfate, and chloride in Antarctic stratospheric aerosols, *J. Geophys. Res.*, *94*, 11,271–11,284, 1989.

Pueschel, R. F., G. V. Ferry, K. G. Snetsinger, J. Goodman, J. E. Dye, D. Baumgardner, and B. W. Gandrud, A case of type I polar stratospheric cloud formation by heterogeneous nucleation, *J. Geophys. Res.*, this issue.

Pruppacher, H., and M. Neiburger, The effect of water soluble substances on the supercooling of water drops, *J. Atmos. Sci.*, *20*, 376–385, 1963.

Salawitch, R. J., G. P. Gobbi, S. C. Wofsy, and M. B. McElroy, Denitrification in the Antarctic stratosphere, *Nature*, *339*, 525–527, 1989

Schlager, H., F. Arnold, D. Hofmann, and T. Deshler, Balloon observation of nitric acid aerosol formation in the arctic stratosphere, I, Gaseous nitric acid, *Geophys. Res. Lett.*, *17*, 1275–1278, 1990.

Solomon, S., R. R. Garcia, F. S. Rowland, and D. J. Wuebbles, On the depletion of Antarctic ozone, *Nature*, *321*, 755–758, 1986.

Steele, H. M., and P. Hamill, Effects of temperature and humidity on the growth and optical properties of sulphuric acid-water droplets in the stratosphere, *J. Aerosol Sci.*, *12*, 517–528, 1981.

Steele, H. M., P. Hamill, M. P. McCormick, and T. J. Swissler, The formation of polar stratospheric constituents over Antarctica during September, *J. Geophys. Res.*, *88*, 2055–2067, 1983.

Taesler, I., R. G. Delaplane, and I. Olovson, Hydrogen bond studies, XCIV, Diaquaoxonium ion in nitric acid trihydrate, *Acta Crystallogr., Sect B.*, *31*, 1489–1495, 1975.

Toon, O. B., P. Hamill, R. P. Turco, and J. Pinto, Condensation of HNO_3 and HCl in the winter polar stratospheres, *Geophys. Res. Lett.*, *13*, 1284–1287, 1986.

Toon, O. B., R. P. Turco, J. Jordan, J. Goodman, and G. Ferry, Physical processes in polar stratospheric ice clouds, *J. Geophys. Res., 94*, 11,359–11,380, 1989.

Toon, O. B., E. V. Browell, S. Kinne, and J. Jordan, An analysis of lidar observations of polar stratospheric clouds, *Geophys. Res. Lett., 17*, 393–396, 1990.

Turco, R., A. Plumb, and E. Condon, The Airborne Arctic Stratospheric Experiment: Proloque, *Geophys. Res. Lett., 17*, 313–316, 1990.

Wilson, J. C., M. Loewenstein, D. W. Fahey, B. Gary, S. D. Smith, K. K. Kelly, G. V. Ferry, and K. R. Chan, Observations of condensation nuclei in the Airborne Antarctic Ozone Experiment: Implications for new particle formation and polar stratospheric cloud formation, *J. Geophys. Res., 94*, 16,437–16,448, 1989.

Wilson, J. C., M. R. Stolzenburg, W. E. Clark, M. Loewenstein, G. V. Ferry, and K. R. Chan, Measurements of condensation nuclei in the Airborne Arctic Stratospheric Expedition: Observations of particle production in the polar vortex, *Geophys. Res. Lett., 17*, 361–364, 1990.

Wofsy, S. C., G. P. Gobbi, R. G. Salawitch, and M. B. McElroy, Nucleation and growth of HNO_3 $3H_2O$ particles in the polar stratosphere, *J. Atmos. Sci., 47*, 2004–2012, 1990.

Zerull, R. H., Scattering measurements of dielectric and absorbing nonspherical particles, *Beit. Phys. Atmos., 49*, 168–188, 1976.

D. Baumgardner, J. E. Dye, and B. W. Gandrud, National Center for Atmospheric Research, P. O. Box 3000, Boulder, CO 80307.

K. R. Chan, G. V. Ferry, and M. Loewenstein, NASA Ames Research Center, Moffett Field, CA 94035.

B. L. Gary, Jet Propulsion Laboratory, Pasadena, CA 91109.

S. R. Kawa and K. K. Kelly, NOAA Aeronomy Laboratory, Boulder, CO 80303.

(Received March 6, 1991;
revised October 30, 1991
accepted October 30, 1991)